Design principles of collateral sensitivity-based dosing strategies

Linda B. S. Aulin[1*], Apostolos Liakopoulos[2], Piet H. van der Graaf[1,3], Daniel E. Rozen[2], J. G. Coen van Hasselt[1*]

1. Leiden Academic Centre for Drug Research, Leiden University, Leiden, The Netherlands

2. Institute of Biology, Leiden University, Leiden, The Netherlands

3. Certara, Canterburry, United Kingdom

*Corresponding authors:

Linda Aulin, l.b.s.aulin@lacdr.leidenuniv.nl, Leiden University, Einsteinweg 55, 2333 CC, Leiden, The Netherlands

Coen van Hasselt, coen.vanhasselt@lacdr.leidenuniv.nl, Leiden University, Einsteinweg 55, 2333 CC, Leiden, The Netherlands

Abstract: 148/150

Manuscript: 5064/5000

Figures: 10

Tables: 2

References: 39

Supplemental material: 5 Figures

Keywords: collateral sensitivity, pharmacodynamics, antimicrobial resistance

Abstract

Collateral sensitivity (CS)-based antibiotic treatments, where increased antibiotic resistance to one antibiotic leads to increased antibiotic sensitivity of second antibiotic, could constitute a strategy to limit emergence of antibiotic resistance. However, it is unclear how to design CS-based dosing schedules that effectively suppress resistance. Here, we use a mathematical modelling approach incorporating pharmacokinetic and pharmacodynamic features to simulate bacterial population dynamics for different combination treatment designs. We study how differences in pathogen- and drug-specific factors influence the probability of resistance at end of treatment for different dosing strategies. We show that drug administration sequence is critical, whilst surprisingly, reciprocal CS was not essential to suppress resistance. Overall, we find that one-day cycling or simultaneous treatment schedules were most effective to supress the probability of resistance. In conclusion, our analysis provides insight into key design principles that contribute to the success of CS-based treatment strategies in suppressing resistance.

Funding

This work is funded by ZonMW Off Road (Project number 451001033) and NWA Idea Generator (Project number NWA.1228.192.140). AL and DER were supported through the JPI-EC-AMR (Project 547001002).

Introduction

Antimicrobial resistance (AMR) is a worldwide health threat due to the reduction of clinically effective antibiotics. Current drug discovery pipelines of new-in-class antibiotic agents are insufficient to offset the emergence of new AMR[1]. Innovative strategies to reduce the rate that AMR develops are thus critically needed. Treatment with antibiotics in individual patients represents one important situation where *de novo* AMR may emerge[2,3]. However, antibiotic dosing strategies used in the clinic do not typically explicitly consider within-host emergence of AMR. Instead, current clinical strategies are primarily based on exposure targets that are associated with sufficient bacterial kill in preclinical studies, or with clinical outcomes in patient studies[4]. Thus, there is need for clinical dosing strategies designed to suppress emergence of AMR[5].

Selection inversion mechanisms that exploit evolutionary trade-offs associated with AMR are of increasing interest to design antibiotic dosing strategies that suppress the within-host emergence of AMR [6]. In this context, collateral sensitivity (CS), where resistance to one antibiotic leads to increased sensitivity to a second antibiotic, has been proposed as a potential strategy to suppress AMR [7,8]. CS has been extensively characterized *in vitro*, typically by evolving AMR strains and then quantifying correlated changes in the sensitivity to other antibiotics[9–12]. CS effects have been characterized for several clinically relevant pathogens, including *Escherichia coli*[9,13], *Pseudomonas aeruginosa*[14], *Enterococcus faecalis*[13], *Streptococcus pneumoniae*[15], and *Staphylococcus aureus*[16]. CS relationships between antibiotics can either be one directional, where decreased sensitivity to one antibiotic show CS to a second antibiotic but not the reverse, or reciprocal, where decreased sensitivity either of the antibiotics results in CS to the other. Reciprocal CS is often considered a prerequisite for effective CS-based treatments, but such relationships have been less frequently observed compared to one directional CS[9–16].

CS-based treatment strategies can use different designs to combine antibiotics showing a CS-relationship, including simultaneous, sequential, or cyclic (alternating) administration. For example, consider a cycling drug strategy using two antibiotics showing reciprocal CS (**Figure 1**). Initial treatment would start with antibiotic A. This leads to resistance to A and a corresponding increase in sensitivity to B. When treatment is switched to antibiotic B, the inverted selection pressure leads to the eradication of cells that are resistant to antibiotic A (due to CS), but possibly favouring any remaining cells that are resistant to B, but susceptible to antibiotic A. . By cycling between the two drugs to sequentially eliminate all cells that show reciprocal CS, complete eradication can been achieved. Although the conceptual strategies of CS-based treatments have been discussed[6], it remains unclear when CS-based dosing strategies are most likely to be beneficial, and how to design specific antibiotic dosing (combination) schedules based on CS. Furthermore, it is unclear how pathogen-specific factors, such as CS effect magnitude and directionality, fitness costs of resistance, and mutation rates, as well as pharmacological factors related to pharmacokinetics (PK) and pharmacodynamics (PD) for different drug types, can affect optimal dosing schedules.

Experimental studies *in vitro* are essential to characterize the incidence, evolvability and magnitude of CS, all of which are important but isolated components that may contribute to the success of CS-based treatments [9–16]. However, for translation of *in vitro* CS findings to *in vivo* or clinical treatment scenarios, consideration of pharmacodynamic (PD)

and pharmacokinetic (PK) factors is essential, as these determine the differential impact of different antibiotics on the rate and concentration dependent effects of bacterial growth, inhibition, and killing [17,18]. By affecting bacterial dynamics, antibiotic PK-PD can have a profound influence on resistance evolution, and are therefore key factors to design optimised CS-informed treatments. To this end, mathematical models are important tools to integrate multiple biological and pharmacological factors contributing to treatment outcomes, including different PK parameters of specific antibiotics in patients, antibiotic-specific PD parameters, and pathogen specific characteristics such as strain fitness and the rate and magnitude of CS effects.

In the current study we aim to determine if and when CS-based dosing schedules are likely to lead to the suppression of within-host emergence of antibiotic resistance. We utilise a mathematical modelling approach to comprehensively study the influence of key pathogen-specific factors and the contribution of PK and PD properties to identify key design principles to inform rational design of antibiotic combination dosing schedules that suppress antibiotic resistance.

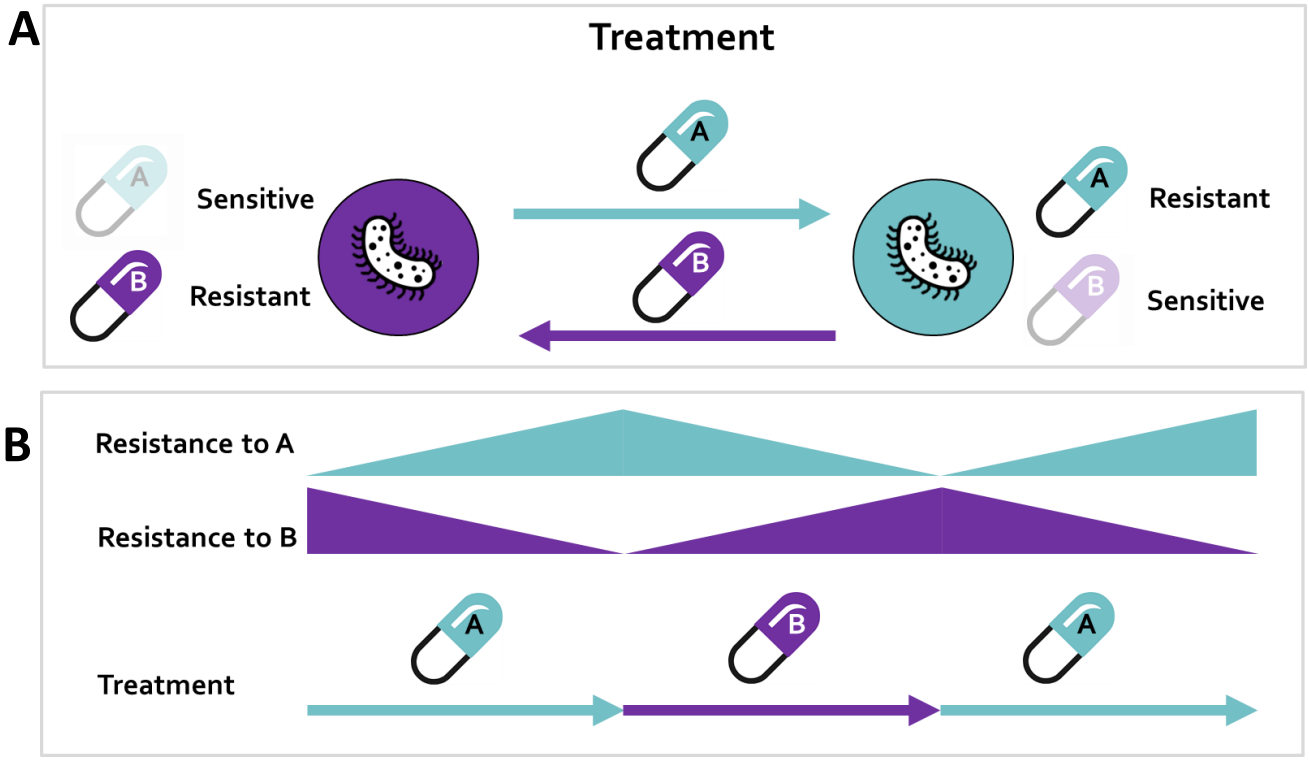

Figure 1. Concept of collateral sensitivity (CS)-based treatments using two hypothetical drugs, antibiotic A and B. Adapted from Pál et al 2015 [19] **A:** Reciprocal CS relationship between antibiotic A and B. **B:** Theoretical cycling regimen exploiting CS between antibiotic A and B to supress resistance.

Methods

Model framework

A differential-equation based model of components accounting for antibiotic PK and PD, and associated bacterial population dynamics, to study the impact of differences in pathogen- and drug-specific characteristics for different treatment strategies for treatment with two antibiotics (AB) referred to as antibiotic A (AB_A) and antibiotic B (AB_B).

Pharmacokinetics

A mono-exponential PK model was defined for both antibiotics AB_i, where i = {A,B}, as follows:

$$\frac{dA_{AB_i}}{dt} = -k_{e,AB_i} \times A_{AB_i} \quad (1)$$

$$t_{half,AB_i} = \frac{ln(2)}{k_{e,AB_i}} \quad (2)$$

$$C_{AB_i} = \frac{A_{AB_i}}{V_{AB_i}} \quad (3)$$

where **Equation 1** describes the change of the amount of AB_i over time after intravenous administration, k_{e,AB_i} is the elimination rate of AB_i, which can also be expressed as a half-life (t_{half,AB_i}) (**Equation 2**). The plasma concentration (C_{AB_i}), which is the assumed driver of the antibiotic effect, is calculated using the V_{AB_i}, the distribution volume of AB_i (**Equation 3**).

Bacterial subpopulations

A model for antibiotic sensitive and resistant subpopulations was defined, comprising of a four-state stochastic hybrid ordinary differential equation (ODE) model, where each state represents a bacterial subpopulation with different antibiotic susceptibility towards AB_A and AB_B.

The model included an antibiotic sensitive bacterial subpopulation (WT) (**Equation 4**), one mutant subpopulation resistant to AB_A but sensitive to AB_B (R_A) (**Equation 5**), one mutant subpopulation sensitive to AB_A but resistant to AB_B (R_B) (**Equation 6**), and one double mutant subpopulation resistant to both AB_A and AB_B (R_{AB}) (**Equation 7**). The initial bacterial population was assumed to be homogeneous and in the sensitive WT state unless stated otherwise.

$$\frac{dWT}{dt} = WT \times k_{net,WT}(WT, R_A, R_B, R_{AB}, F_{fit}, n_{WT}) \times E_{AB,WT}(E_{AB_A,WT}, E_{AB_B,WT}) - k_{WT,R_A}(WT, \mu) - k_{WT,R_B}(WT, \mu) \quad (4)$$

$$\frac{dR_A}{dt} = R_A \times k_{net,R_A}(WT, R_A, R_B, R_{AB}, F_{fit}, n_{R_A}) \times E_{AB,R_A}(E_{AB_A,R_A}, E_{AB_B,R_A}) + k_{WT,R_A}(WT, \mu) - k_{R_A,R_{AB}}(R_A, \mu) \quad (5)$$

$$\frac{dR_B}{dt} = R_B \times k_{net,R_B}(WT, R_A, R_B, R_{AB}, F_{fit}, n_{R_B}) \times E_{AB,R_B}(E_{AB_A,R_B}, E_{AB_B,R_B}) + k_{WT,R_B}(WT, \mu) - k_{R_B,R_{AB}}(R_B, \mu) \quad (6)$$

$$\frac{dR_{AB}}{dt} = R_{AB} \times k_{net,R_{AB}}(WT, R_A, R_B, R_{AB}, F_{fit}, n_{R_{AB}}) \times E_{AB,R_{AB}}(E_{AB_A,R_{AB}}, E_{AB_B,R_{AB}}) + k_{R_A,R_{AB}}(R_A, \mu) + k_{R_B,R_{AB}}(R_B, \mu) \quad (7)$$

The above equations (**Equation 4-7**) describe the subpopulation specific rate of change for bacterial density, which is dependent on the bacterial density of subpopulation z, subpopulation specific net growth ($k_{net,z}$), antibiotic effect ($E_{AB,z}$), and mutation transition(s) ($k_{z,M}$) if present.

Resistance mutation

Resistance evolution was included as stochastic mutation process. This process was modelled using a binomial distribution B with a mutation probability equal to the mutation rate (μ). The number of bacteria mutated per time step $k_{z,M}$ depende on the number of bacteria available for mutation (n_z), *i.e.* the bacterial subpopulation density of subpopulation z multiplied by the infection volume V, for mutation at time t (**Equation 8**). Double resistant mutants evolved through two mutation steps.

$$k_{z,M} = \frac{B(n_z,\mu)}{V} \quad (8)$$

Pharmacodynamic effects

Drug effects on bacterial subpopulations (**Equation 4-7**) were assumed to be additive and the total drug effect for each subpopulation *z* ($E_{AB,z}$), and was implemented as follows (**Equation 9**):

$$E_{AB,z} = 1 - \left(E_{AB_A,z}(C_{AB,A}, G_{min,\,AB_A}, Hill_{AB_A}, MIC_{AB_A,\,z}) + E_{AB_B,z}(C_{AB,B}, G_{min,\,AB_B}, Hill_{AB_B}, MIC_{AB_B,\,z})\right) \quad \text{Equation 9}$$

Here, antibiotic-mediated effects were implemented according to a previously developed PD model [17], where the effect of the i^{th} antibiotic on bacterial subpopulation *z* ($E_{AB_i,z}$) related to the unbound antibiotic concentration ($C_{AB,i}$) according to Equation 10.

$$E_{AB_i,z} = \frac{(G_{max} - G_{min,\,AB_i}) \times \left(\frac{C_{AB,i}}{MIC_{AB_i,z}}\right)^{Hill_{AB_i}}}{\left(\frac{C_{AB_i}}{MIC_{AB_i,z}}\right)^{Hill_{AB_i}} - \frac{G_{min,\,AB_i}}{G_{max}}} \quad \text{Equation 10}$$

where $G_{max} = 1$, $G_{min,\,AB_i}$ representing the maximal killing effect for the AB_i, $Hill_{AB_i}$ being the shape factor of the concentration-effect relationship, and $MIC_{AB_i,\,z}$ being the subpopulation-specific MIC of AB_i.

Subpopulation-specific MIC for AB_i was defined according to **Equation 11**. Sensitive bacteria were defined as having a MIC of 1 mg/L (MIC_{WT}) and resistant as 10 mg/L (MIC_R). Because the antibiotic concentrations are expressed as folds times MIC_{WT}, the absolute value of MIC_{WT} is irreverent. However, the ratio between MIC_{WT} and MIC_R is of relevance. A tenfold increase was chosen to represent a significant increase for a biologically plausible scenario. Resistance-related CS effects were included on the two singly resistant mutants (R_A and R_B), and were implemented as a proportional reduction (CS_A and CS_B) of the sensitive MIC (MIC_{WT}). The subpopulation- and antibiotic-specific MICs are stated below:

$MIC_{AB_A,WT} = MIC_{WT}$ and $MIC_{AB_B,WT} = MIC_{WT}$

$MIC_{AB_A,R_A} = MIC_R$ and $MIC_{AB_B,R_A} = MIC_{WT} \times CS_B$

$MIC_{AB_A,R_B} = MIC_{WT} \times CS_A$ and $MIC_{AB_B,R_B} = MIC_R$

$MIC_{AB_A,R_{AB}} = MIC_R$ and $MIC_{AB_B,R_{AB}} = MIC_R$

Fitness effects

We considered resistance-associated fitness cost by including a fitness cost factor (F_{fit}), which introduced a fractional reduction of the growth rate (k_G) for each resistance mutation. The net growth rate was implemented according to **Equation 12**.

$$k_{net,z} = k_G \times \left(1 - \frac{WT + R_A + R_B + R_{AB}}{B_{max}}\right) \times F_{fit}^{n,z} \quad \text{Equation 12}$$

where $k_{net,z}$ is the subpopulation specific net growth in the absents of antibiotic, B_{max} is the systems maximal carrying capacity, and n_z is the subpopulation specific number of mutations (n_z = 0, 1 or 2).

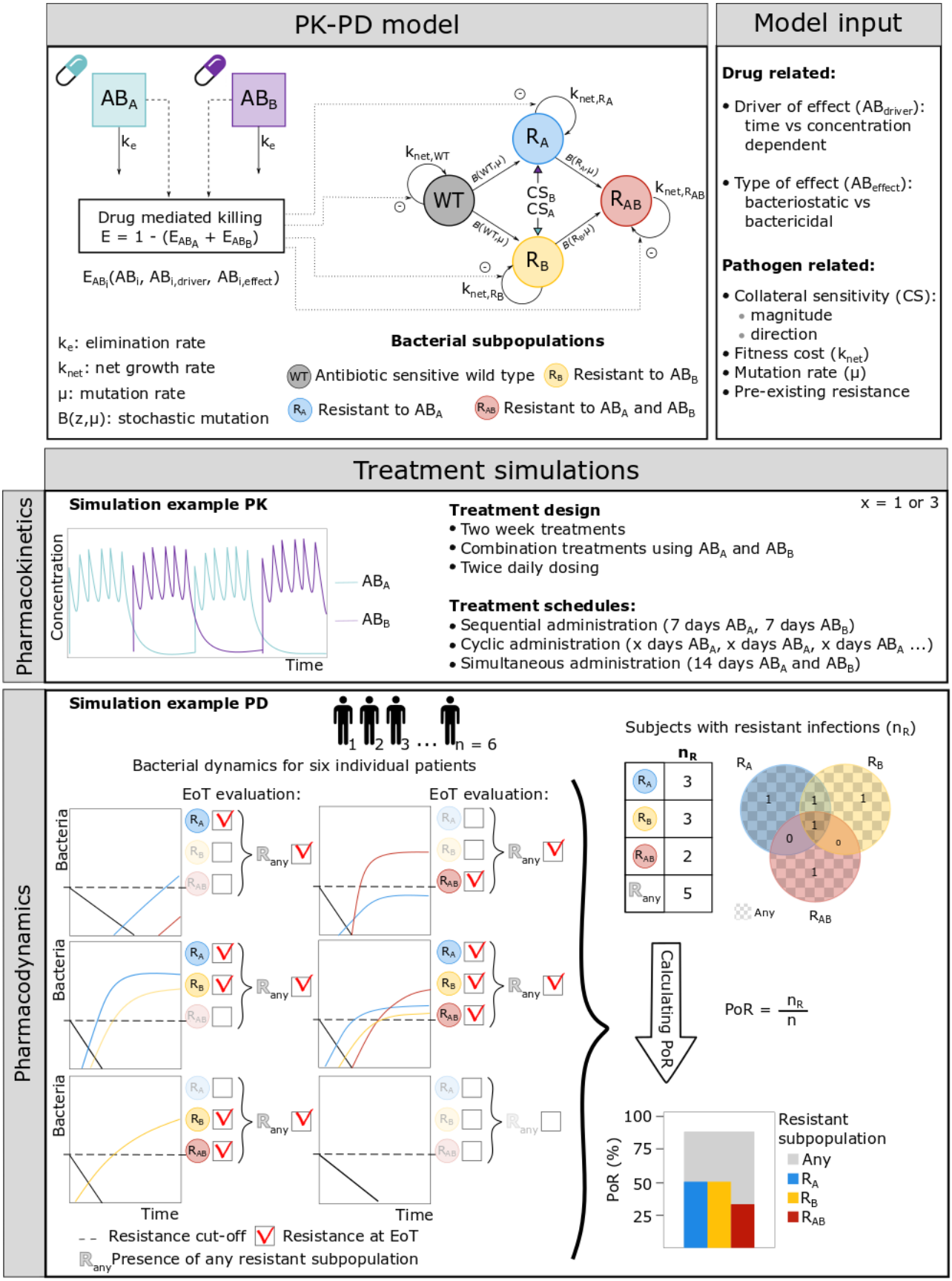

Figure 2. Simulation workflow. Pharmacokinetic-pharmacodynamic (PK-PD) framework comprising of four bacterial subpopulations (WT, R_A, R_B, R_{AB}) and PK-PD of two hypothetical antibiotics (AB_A and AB_B). The framework includes fixed infection- and pathogen-specific parameters and fixed drug PK parameters. The model input includes both drug and pathogen related factors, which vary between different scenarios. The framework was used to simulate different treatment schedules of two week combination treatments using AB_A and AB_B for n patients. In the simulation example a three-day cycling treatment regimen (PK panel) is simulated for six patients. The resulting patient specific bacterial profiles are shown in the PD panel. Resistance was evaluated for each patient and bacterial subpopulation at the end of treatment (EoT), for which the corresponding probability of resistance (PoR) was calculated.

Pathogen- and infection-specific parameters

The infection-specific parameters were chosen to represent a human bacteraemia, thus a typical human blood volume of five litre was used as the infection site volume[20]. An initial bacterial density of 10^4 colony forming units (CFU)/mL was used to represent a severe infection, which reflects an early stage of an established infection[21]. A system carrying capacity limitation (B_{max}) of 10^8 CFU/mL[21] was implemented according to Equation 12. When the maximal carrying capacity is reached, the net growth of the total bacterial population is zero, resulting in a stationary phase. During this phase bacterial replication continues, but is offset by bacterial death at the same rate, thereby still allowing for resistance mutations to occur. Resistance mutation rates of 10^{-6} and 10^{-9} mutations/base pair/hour were chosen to represent a high and a moderate mutation rate scenario, respectively[22].

Table 1. Pathogen-, infection-, and drug-specific model parameters used in the simulations.

Parameter	Value	Unit	Scenario	Reference
Pathogen-specific				
Maximal growth rate (k_G)	0.7	h^{-1}	Doubling time of 1 h	-
Mutation rate (μ)	10^{-6} - 10^{-9}	mut/bp/ h	High to moderate mutation rates	-
Infection-specific				
Starting bacterial density (B_0)	10^4	cfu/ml	*In vivo* bacteraemia day one	[21]
Maximal carrying capacity (B_{max})	10^8	cfu/ml	*In vivo* experiment after 4 days	[21]
Infection site volume (V)	5	L	Total blood volume	[20]
Drug-specific				
Distribution volume of AB_i (V_{AB_i})	1	L	Facilitates conversion from amount to concentration	-
Half-life of AB_i (t_{half,AB_i})	5	h	Clinically relevant short half-life	-

Drug-specific parameters

The two hypothetical antibiotics used for the simulations (AB_A and AB_B) have identical one-compartmental PK with distribution volumes of one litre, five-hour half-lives (Table 1), and no protein binding. The selected half-life represents antibiotics with clinically relevant short half-lives, thereby rapidly reaching steady-state concentrations with minimal accumulation. The drugs were administrated as intravenous bolus doses twice daily over a treatment duration of two weeks. Several different dosing regimens were simulated including monotherapy, sequential dosing, cycling regimens, and simultaneous dosing. For sequential and cycling treatments AB_A was used as the starting drug. The doses used were obtained by calculating the required dose to achieve appropriate average steady state concentration (C_{ss}) relative to the MIC_{WT}. The lowest dose that gave kill or stasis of the WT bacteria within the 24 hours of treatment, but allowed for resistance development during monotherapy, was selected for all dosing regimens except for the simultaneous dosing, for which the dose for the individual antibiotics were reduced by half. Four different PD types were included using different combinations of parameter values of Hill (driver of antibiotic effect) and G_{min} (type of antibiotic effect), and represented 1) time-dependent (Hill = 0.5) or concentration-dependent (Hill = 3) and 2) bacteriostatic (G_{min} = -1)

or bactericidal (G_{min} = -3) antibiotics. The corresponding PK-PD relationship of the four different antibiotic types is shown in **Figure 3**.

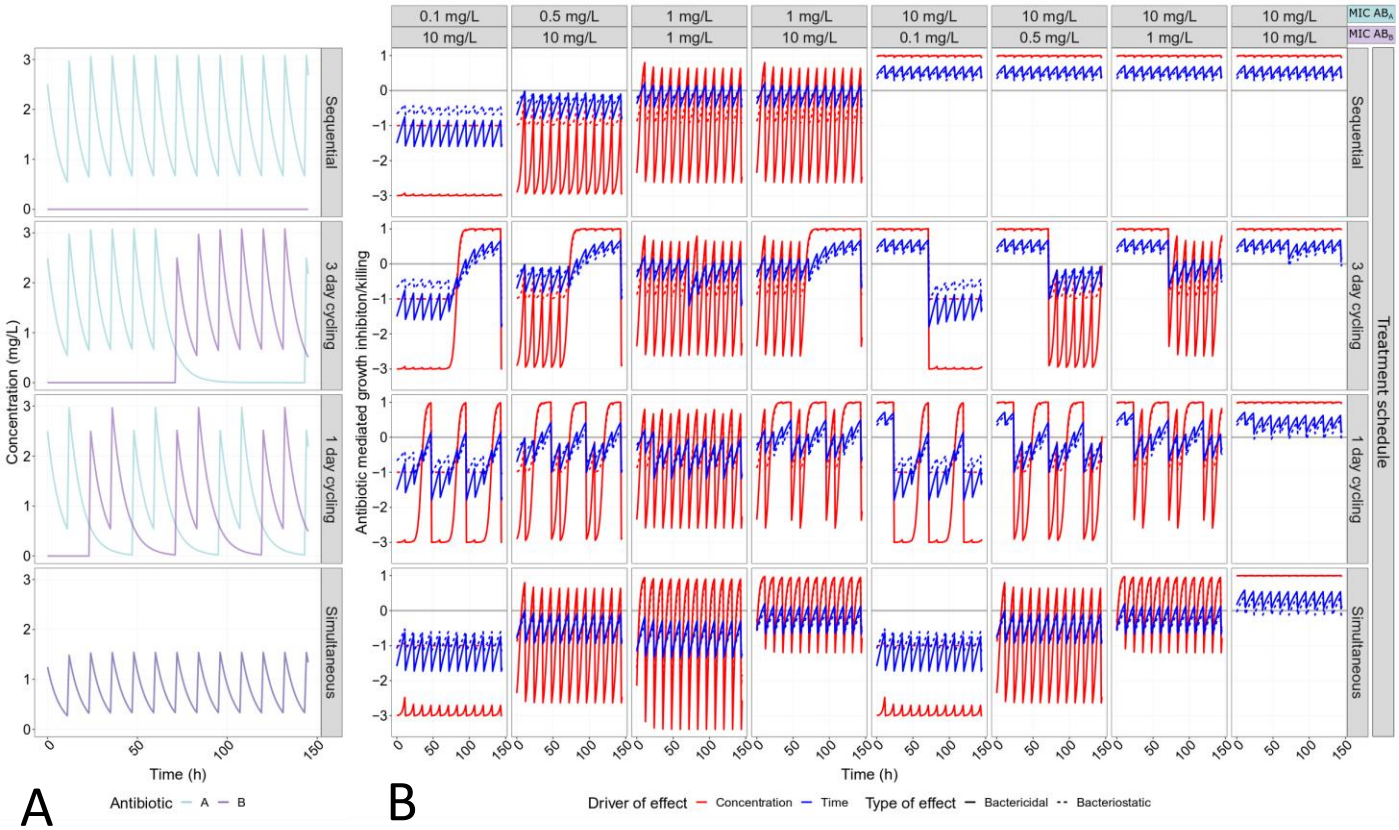

Figure 3. MIC-specific PK-PD relationships. A: Initial pharmacokinetic (PK) profiles of mono or combination treatments using two hypothetical antibiotics AB_A (turquoise) and AB_B (purple), administrated twice daily, with a dose resulting in C_{ss} of 1.5 mg/L or 0.75mg/L for simultaneous dosing. **B**: MIC-specific pharmacodynamic profiles concentration effect relationship of different antibiotic drug types including concentration- (Hill = 3, red) or time- (Hill = 0.5, blue) dependent antibiotics and bactericidal (G_{min} = -3, solid) and bacteriostatic (G_{min} = -1, dashed), where the effect is representing the proportional bacterial growth inhibition/killing. The effect is driven by the PK profile shown in panel A according to Equation 9 and 10.

Simulations scenarios

An initial set of dose finding simulations revealed that monotherapy required C_{ss} equal to 1.5 x MIC_{WT} to achieve killing of the WT, regardless of the drug type used (**Figure S1**). This C_{ss} was subsequently used for treatment scenarios unless explicitly stated otherwise.

We used a systematic simulation strategy to study the impact of CS, fitness cost, initial subpopulation heterogeneity in antibiotic sensitivity, and mutation rate on the probability of resistance (PoR) development for different treatments. An overview of all simulated scenarios can be found in **Table 2**. We simulated treatments using two same-type antibiotics for scenarios without CS as well as in the presence of one directional and reciprocal CS in the magnitude of 50% or 90% reduction of the sensitive MIC (**Table 2**, **Scenario 1** and **2**). For these scenarios the resistance was assumed to occur without any fitness cost, thus allowing us to evaluated CS-specific effect on PoR. We also simulated a set of treatment scenarios using two different antibiotic type in the presence or absence of CS (**Table 2**, **Scenario 3)**. Additionally, we simulated same-type treatment scenarios covering a wide range of fitness costs (10% to 50% per mutation) implemented as a growth rate reduction (**Table 2**, **Scenario 4)**. To assess the impact of therapeutic window of antibiotics, as reflected by the fold-difference of steady state concentration (C_{ss}) to the MIC_{WT}, we simulated

different dosing levels resulting in a range of C_{ss} of 0.5-5 x MIC_{WT} (**Table 2**, **Scenario 5)**. In order to better understand the interplay between CS and fitness cost we simulated these scenarios with and without CS. We further investigated how low levels of pre-existing resistance (1%) towards either AB_A or AB_B affected the PoR at the end of treatment for different dosing regimens (**Table 2**, **Scenario 6)**. Finally, we examined the effect of increased mutation rates on resistance development (**Table 2**, **Scenario 7)**.

Each simulated scenario was realized 500 times (n), thus representing 500 virtual patients.

Table 2. Simulation scenarios evaluated and associated pathogen- and pharmacological factors studied

Scenario	Pathogen factors				Treatment factors	
	Collateral sensitivity (%)	Fitness cost per mutation (%)	Mutation rate (mut/bp/h)	Pre-existing resistance	PD parameters	Steady state concentration*
1: Treatment design	Symmetric reciprocal: 50 or 90	No	10^{-9}	No	Same-type combinations: $G_{min,AB_A} = G_{min,AB_B}$ and $Hill_{AB_A} = Hill_{AB_B}$	1.5x MIC_{WT}
2: Directionality of CS	One directional or asymmetric reciprocal: 50 or 90	No	10^{-9}	No	Same-type combinations: $G_{min,AB_A} = G_{min,AB_B}$ and $Hill_{AB_A} = Hill_{AB_B}$	1.5x MIC_{WT}
3: Drug sequence	Symmetric reciprocal: 50 or 90	No	10^{-9}	No	Different types combined: $G_{min,AB_A} \neq G_{min,AB_B}$ and/or $Hill_{AB_A} \neq Hill_{AB_B}$	1.5x MIC_{WT}
4: Fitness cost	Symmetric reciprocal: 50 or 90	Yes: 10, 20, 30, 40, or 50	10^{-9}	No	Same-type combinations: $G_{min,AB_A} = G_{min,AB_B}$ and $Hill_{AB_A} = Hill_{AB_B}$	1.5x MIC_{WT}
5: Therapeutic window	Symmetric reciprocal: 50 or 90	No	10^{-9}	No	Same-type combinations: $G_{min,AB_A} = G_{min,AB_B}$ and $Hill_{AB_A} = Hill_{AB_B}$	0.5-5x MIC_{WT}
6: Pre-existing resistance	Symmetric reciprocal: 50 or 90	No	10^{-9}	Yes: 1% R_A or 1% R_B	Same-type combinations: $G_{min,AB_A} = G_{min,AB_B}$ and $Hill_{AB_A} = Hill_{AB_B}$	1.5x MIC_{WT}
7: Mutation rate	Symmetric reciprocal: 50 or 90	No	10^{-9}, 10^{-8}, 10^{-7}, or 10^{-6}	No	Same-type combinations: $G_{min,AB_A} = G_{min,AB_B}$ and $Hill_{AB_A} = Hill_{AB_B}$	1.5x MIC_{WT}

CS=Collateral sensitivity; PD=Pharmacodynamics; $G_{min,ABi}$ = type of antibiotic effect; $Hill_{ABi}$ = driver of antibiotic effect; MIC_{WT} = 1 mg/L

*divided by 2 for simultaneous dosing regimens

Evaluation metrics

For evaluation of the simulated scenario's we computed the probability of resistance (PoR), which was defined as resistant bacteria reaching at the end of treatment at least the initial bacterial density of 10^4 CFU/mL, for each population separately (Equation 13)

$$PoR_z = \frac{n_{R,z}}{n} \quad (13)$$

where $n_{R,z}$ denotes the number of patients having resistant bacteria of subpopulation z at the end of treatment (Equation 14):

$$n_{R,z} = \sum_{k=1}^{n} \mathbf{1}_{x_{z,k} \geq 10^4} \quad (14)$$

where **1** denotes the indicator function and $x_{z,k}$ denotes the bacterial density of subpopulation z at the end of treatment of patient k.

Furthermore we also calculated the PoR for the case where any, i.e., one or more resistant subpopulation(s) exceeded the resistance cut-off (R_{Any}).

The standard error (SE) of the PoR was calculated according to **Equation 15**.

$$SE = \sqrt{\frac{PoR(1-PoR)}{n}} \quad (15)$$

Software and model code

All analyses were conducted in R version 4.0.4, using the ODE solver package RxODE (version 1.0.0-0)[23,24]. The associated model code is available at https://github.com/vanhasseltlab/CS-PKPD).

Results

Drug type and treatment schedule influence the probability of resistance

We simulated antibiotic combination treatments of two antibiotics from the same type, with either no (0%) or reciprocal CS (50 or 90% decrease of MIC_{WT}). We show that the impact of reciprocal CS on resistance dynamics is dependent on the simulated drug type and dosing regimen (**Figure 4**). Treatments with concentration dependent antibiotics could achieve full CS-based resistance suppression for dosing schedules using one-day cycling interval (**Figure 4C, 4G**) or simultaneous administration (**Figure 4D, 4H**). A 50% MIC reduction was sufficient to achieve this effect for three out of the four treatments, which is relevant in light of experimental results consistent with these CS magnitudes. Treatments using time dependent antibiotics dosed according to these schedules (**Figure 4K, 4L, 4O, 4P**)

were efficient in fully supressing resistance with or without CS. Full resistance suppression was not achieved by any of the other treatment schedules tested. Although none of the CS-based treatments dosed according to the three-day cycling regimen managed to fully supress resistance, the ones using time dependent antibiotics (**Figure 4J, 4N**) did show reduced PoR in presence of CS. For these treatments, the effect of CS was most prominent for the bacteriostatic antibiotics (**Figure 4N**) where a CS magnitude of 90% resulted in ΔPoR -29.2%. Such a decreased could have a potential clinical benefit. Importantly, we also find that for some treatments the presence of CS was not only unable to fully supress resistance, but favoured the formation of double resistant mutants (**Figure 4E, 4F, 4I, 4M).**

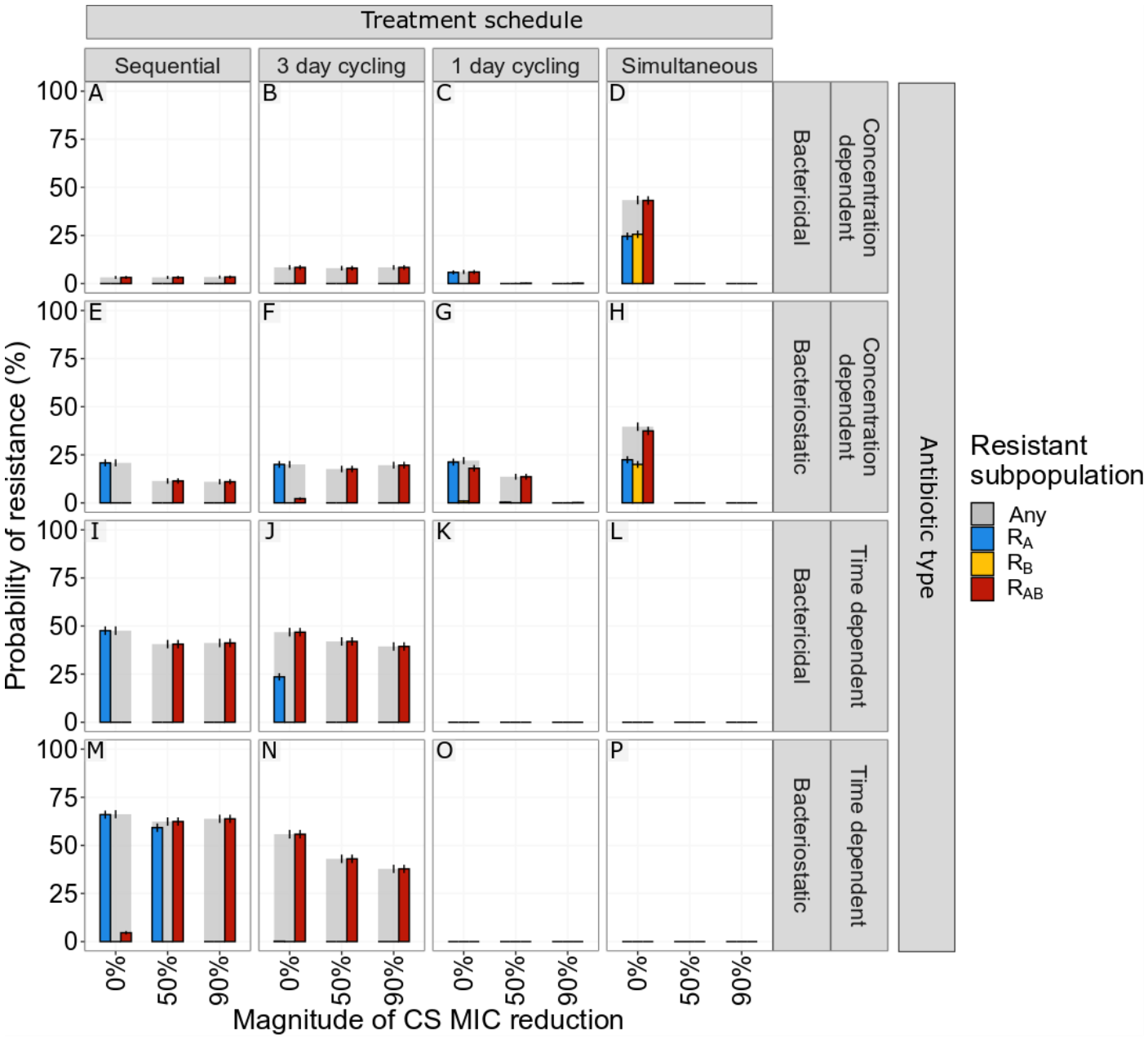

Figure 4. The effect of treatment design and antibiotic in relation to different levels of collateral sensitivity (CS) on the probability of resistance (PoR) at end of treatment. The simulations show that CS had a profound impact on resistance development for treatments with concentration dependent antibiotics with one-day cycling interval or simultaneous administration. PoR was estimated at end of treatment for treatments using different designs (columns) and antibiotic types (rows). Subpopulation-specific PoR are indicated by different colour and R_{Any}, defined as the presence of any resistant subpopulation, is indicated in grey. The error bars represent the standard error of the estimation of PoR.

Directionality of CS effects influence the probability of resistance

We next sought to determine if reciprocity is a requirement for CS-based treatments to suppress *de novo* resistance. We find that bactericidal and bacteriostatic drugs showed the same overall behaviour for the treatment tested when related to CS directionality (**Figure S2**). We specifically focus on the one-day cycling and simultaneous treatment that appeared to be most successful in fully supressing resistance development for reciprocal CS. We find that for the one-day cycling regimen the presence of one directional CS for the second administrated antibiotic (AB_B) is sufficient to fully suppress resistance development. This is illustrated for treatments using concentration dependent bacteriostatic antibiotic in **Figure 5**. In this scenario, one directional CS results in resistance levels close to the reciprocal scenario (*e.g.*, one directional CS resulted in 2.2% PoR of R_{Any} for bacteriostatic (Figure 5A) vs 0.2% for reciprocal CS (Figure 5B)). In contrast, when CS is only present for the first antibiotic (AB_A) administered, we found resistance levels close to the scenario without any CS (PoR 7.2% (Figure 5D) vs 6.0% (Figure 5C)). Overall, these results suggest that when designing CS-based one-day cycling treatments using a drug-pair without reciprocity, the order for which these are administrated has a large impact on treatment success and the therapy should be initiated with the antibiotic for which there is no CS. This strategy allows for evolution and growth of R_A on the first day, while R_B is supressed by AB_A. When the selection is inverted on day two, the low levels of R_A present is effectively killed by AB_B in the presence of CS. In the absence of CS towards AB_B, R_A will reach high levels, which can lead to further evolution of the R_{AB}. When simultaneous administration of concentration-dependent antibiotics is used, we found that reciprocity is necessary to fully supress resistance, as one directional CS will only supress resistance for the resistant subpopulation which show CS (**Figure 5A and 5B**). However, one directional CS did reduce the PoR for R_{Any} by approximately 50% (ΔPoR -18.4% and 20.2% for CS_A and CS_B, respectively) for both of these treatments, thus having a potential clinical value.

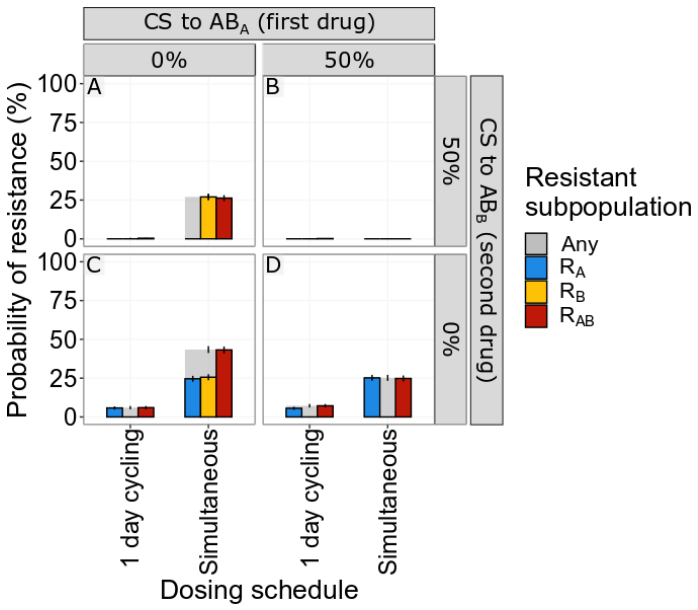

Figure 5. The effect of the direction or reciprocally of collateral sensitivity (CS) on end of treatment probability of resistance (PoR). PoR was estimated at end of treatment for different CS scenarios using concentration dependent bacteriostatic drugs. Subpopulation-specific PoR is indicated by different colour and R_{Any} resistance, defined as the presence of any resistant subpopulation, is indicated in grey. The error bars represent the standard error of the estimation of PoR. For the one-day cycling regimen it became evident that the CS towards the second administrated drug (AB_B) was driving the effect, CS-based dosing using simulations administration of concentration dependent antibiotics showed that reciprocity is necessary to supress overall resistance.

Administration sequence and antibiotic type influence resistance suppression

As CS dose not only occur between antibiotics of the same type, it is important to understand how the administration sequence of different-type antibiotics affect resistance evolution in the presence of reciprocal CS. Our results for one-day cycling and simultaneous schedules demonstrated that the suppression of *de novo* resistance was mainly driven by the first administrated antibiotic (AB_A) for all non-simultaneous regimens (**Figure S3**), highlighting the importance of drug sequence. In line with our findings for same-type antibiotic combination treatments (**Figure 4**), resistance was fully suppressed from CS only when using one-day cycling or simultaneous administration dosing regimens. Particularly for one-day cycling regimens (**Figure 6**), initiating treatment with a time-dependent antibiotic was more effective at supressing resistance in the presence of reciprocal CS compared to the initial administration of a concentration dependent antibiotic.

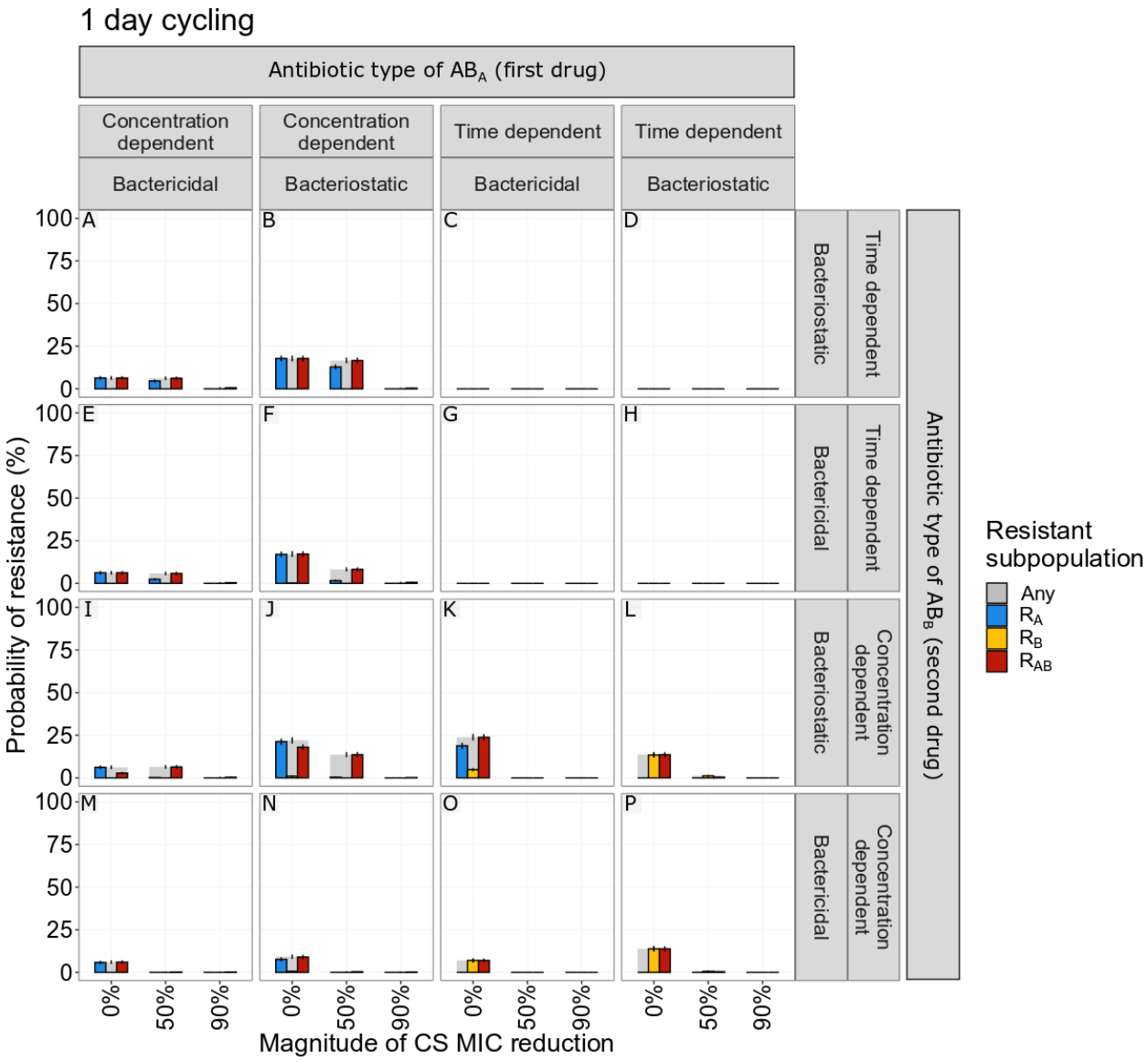

Figure 6. The effect of using different antibiotic combinations during one-day cycling treatments in relation to different levels of collateral sensitivity (CS) on the probability of resistance (PoR) at the end of treatment. The simulations showed that initiating treatment with a time dependent than with a concentration dependent antibiotic was more effective in supressing resistance in the presence of reciprocal CS. PoR was estimated at the end of treatment for one-day cycling regimen with different antibiotic combinations. Subpopulation-specific PoR is indicated by different colour and R_{Any}, defined as the presence of any resistant subpopulation, is indicated in grey. The error bars represent the standard error of the estimation of PoR.

CS-based combinations show greatest promise for antibiotics with a narrow therapeutic window

Although many antibiotics are well-tolerated and can be dosed well above the MIC of susceptible strains others, *e.g.*, aminoglycosides, display a narrow therapeutic window due to toxicity[25–27]. Understanding the relationship between average steady-state concentrations (C_{ss}) and the impact of CS on *de novo* resistance development would help identify which clinical scenarios that CS could be exploited to improve treatment. A set of simulated dosing regimens with same-type antibiotics resulting in C_{ss} between 0.5-5 x MIC_{WT} revealed that CS has the greatest impact on R_{Any} for C_{ss} close to the MIC_{WT} (**Figure 7** and **S4**). Most treatments showing a benefit of CS lost the advantage when the C_{ss} exceeded 1.5 x MIC_{WT}. The only exception was one-day cycling treatment using concertation dependent bacteriostatic drugs, which retained an advantage up to C_{ss} of 2 x MIC_{WT} (**Figure 7G**).

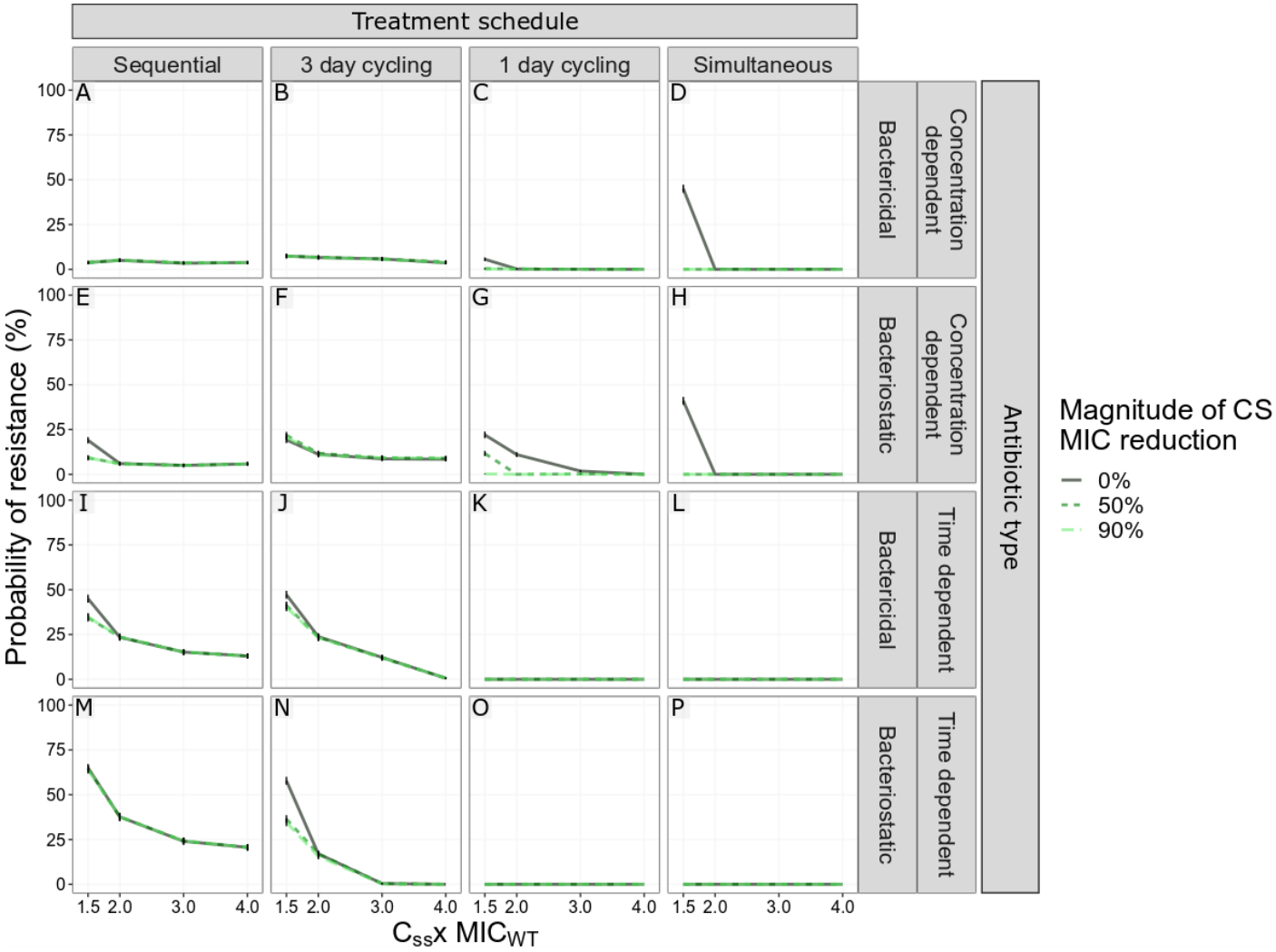

Figure 7. The effect of antibiotic steady state concentrations (C_{ss}) in relation to different levels of collateral sensitivity (CS) on the probability of resistance at the end of treatment (PoR). The simulation revealed that CS had the largest impact on PoR for C_{ss} close to MIC of the wild type strain (MIC_{WT}). C_{ss} was expressed as factor difference from the MIC_{WT}. PoR of R_{Any}, defined as the presence of any resistant subpopulation, was estimated at the end of treatment for treatments using different designs (columns) and antibiotic types (rows). Colour and line-type indicate the magnitude of reciprocal CS simulated. The error bars represent the standard error of the estimation.

Fitness cost of antibiotic resistance can contribute to the success of CS-based treatments

Resistance evolution is commonly associated with fitness costs.[28]. We studied the impact of different levels of fitness cost on the suppression of *de novo* resistance development (**Figure 8**). Fitness cost was included as a fractional reduction of growth per mutation, thereby doubly penalising the double resistant mutant R_{AB}. In the absence of CS, fitness cost below 50% per mutation had little impact (ΔPoR > -5%) on R_{Any} for most treatment scenarios, except for the three-day cycling regimen using time dependent bacteriostatic drugs (**Figure 8N**), which showed a clear relationship between increasing fitness cost and deceasing R_{Any}. The presence of fitness costs increased the impact of CS on PoR for a number of treatments, including three-day cycling regimen using time dependent antibiotics (**Figure 8J and 8N**) and one-day cycling with concentration dependent bacteriostatic drugs (**Figure 8G**). In the case of these three-day cycling regimens, which failed to fully supress resistance in the presence of fitness cost-free CS, the impact of fitness differed between bactericidal and bacteriostatic drug (**Figure 8J vs 8N**). The fitness cost generating the largest impact of CS (90%)for these treatments on PoR was 20% and 40% cost per mutation when treated with bacteriostatic (Δ PoR -35.0) and bactericidal (Δ PoR -43.8%) drug, respectively.

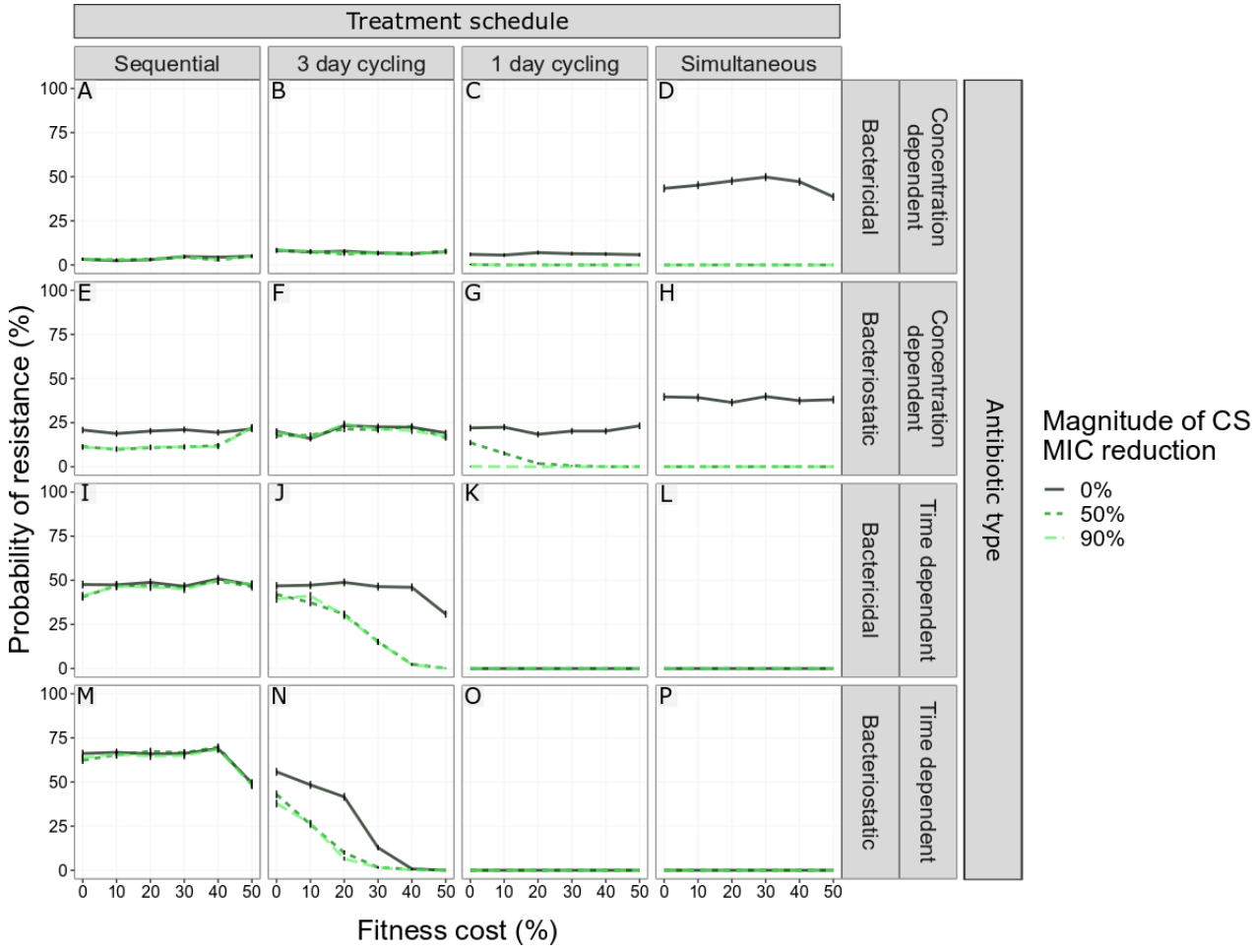

Figure 8. The effect of fitness costs for developing resistance for different levels of collateral sensitivity effects on the probability of resistance (PoR). PoR of R_{Any}, defined as the presence of any resistant subpopulation, was estimated at end of treatment for treatments using different designs (columns) and antibiotic types (rows). Colour and line-type indicate the magnitude of reciprocal CS simulated. The error bars represent the standard error of the estimation of PoR.

CS-based simultaneous treatment designs suppress pre-existing resistance

The presence of a low-number pre-existing resistant cells amongst the bacterial population establishing an infection is a clinically realistic scenario associated with antibiotic-treatment failure[29]. We here studied if CS-based dosing schedules can be used to eradicate such a heterogeneous population **(Figure 9 and S5**). In the absence of CS, the pre-existence of a subpopulation of either single mutant, resulted in higher probability of the expansion and fixation of these resistant populations. As with de novo resistance and cycling regimens, the benefit of reciprocal CS was only apparent when resistance was towards the second antibiotic (R_B). This is illustrated with the one-day cycling treatments shown in Figure 9, where all CS-based treatments could supress PoR for pre-existing R_B, but for failed for all with pre-existing R_A. For three day cycling of concentration dependent drugs and pre-existing resistance towards the first antibiotic, CS was shown to increase the PoR (**Figure S5**). In the presence of CS, all simultaneously dosed treatments were effective in fully suppressing resistance regardless of pre-existing resistance **.**

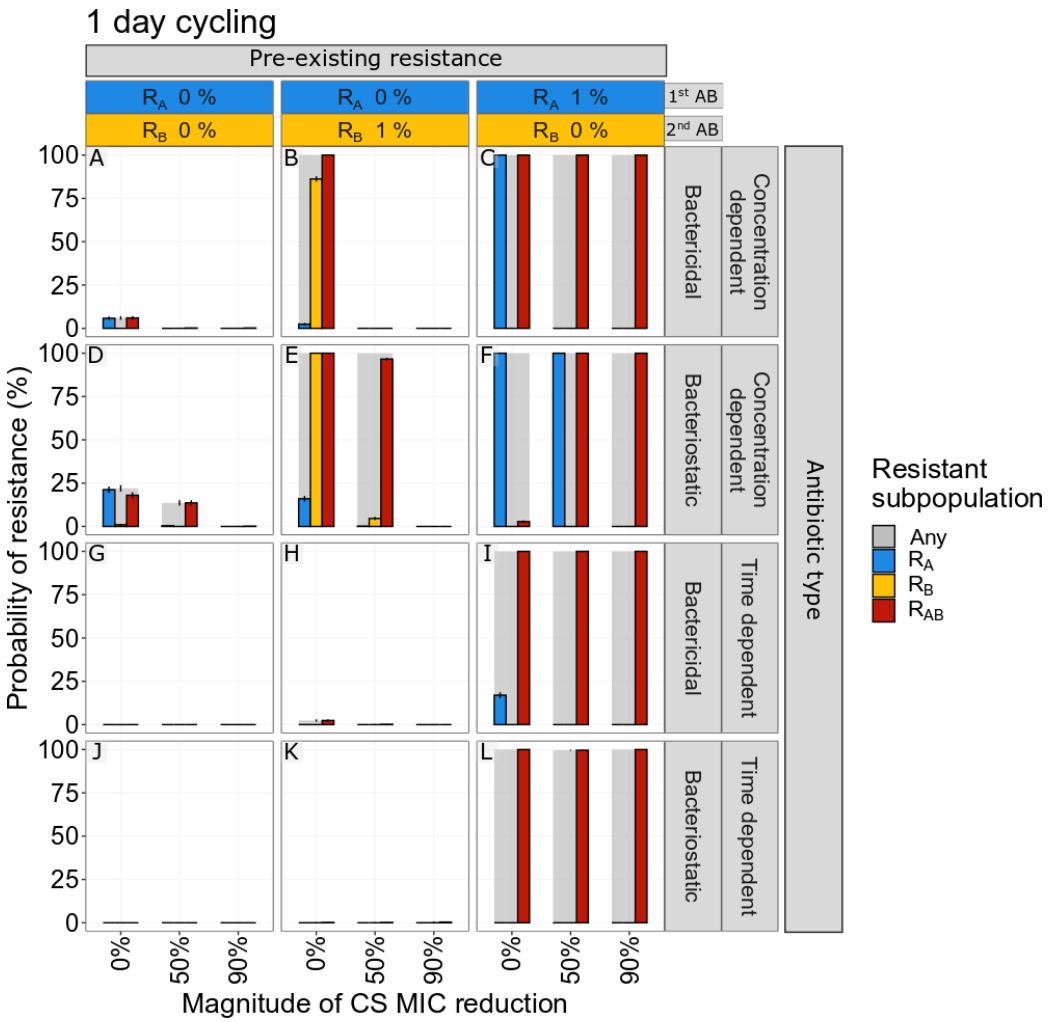

Figure 9. The effect of pre-existing resistant mutants for different magnitudes of collateral sensitivity on the probability of resistance (PoR). PoR was estimated at the end of treatment for different scenarios of low levels of pre-existing resistance (columns) and antibiotic types (rows). Subpopulation-specific probability of resistance is indicated by colour and PoR of R_{Any}, defined as the presence of any resistant subpopulation, is indicated in grey. The error bars represent the standard error of the estimation of PoR.

The combined effect of CS and mutation rate on resistance development differs between treatments

Because some antibiotic treatments can enhance the genome-wide mutation rate in pathogenic bacteria [30], we included a set of simulations with higher mutation rates than 10^{-9} mutations/bp/h (10^{-8}-10^{-6} mutations/bp/h). We show that the impact of mutation rate on the PoR was dependent on the combination of treatment design and the antibiotic type used, especially in the presence of CS (Figure 10). The largest impact of the interaction between CS and mutation on PoR was found for the extremes of the time between switching of antibiotics, *i.e.,* one-day cycling and sequential treatment design (maximum ΔPoR -71.6% and -52.0%, respectively). In the absence of CS an increased mutation rate generally led to an increased PoR, with the exception of simultaneous administration of time-dependent antibiotics, which actually resulted in full suppression of resistance regardless of CS and mutation rate. For some sequential treatments with reciprocal CS (Figure 10E, 10I), the highest PoR was observed at a mutation rate of 10^{-7} mutations/bp/hour, and decreased at higher mutation rates. For all mutation rates and in the presence of CS, simultaneous treatments conferred resistance suppression.

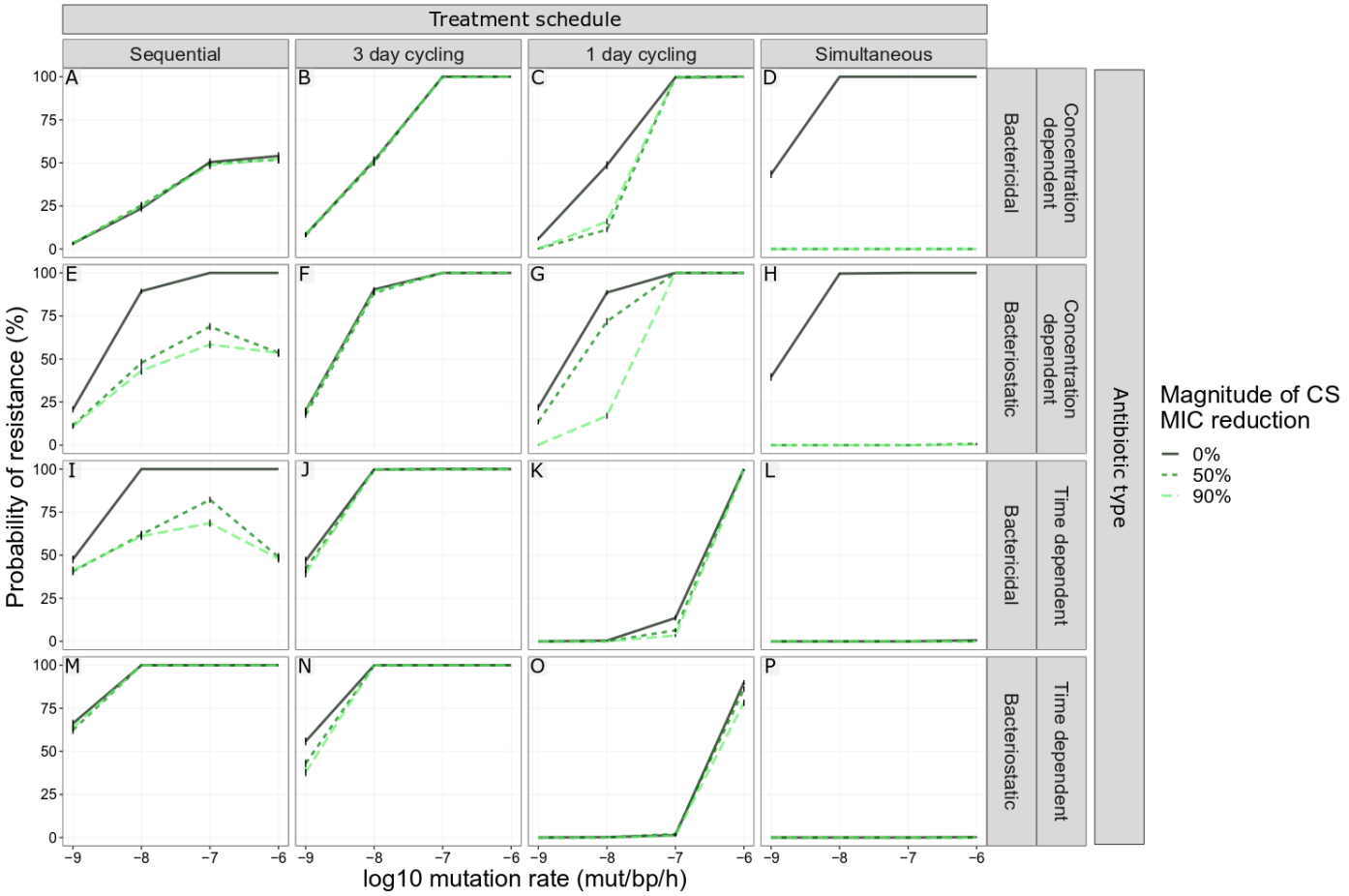

Figure 10. The effect of increased mutation rate for different CS magnitudes on the probability of resistance (PoR). The combined impact of mutation rate and the CS on PoR was dependent on treatment schedule. PoR of R_{Any}, defined as the presence of any resistant subpopulation, was estimated at the end of treatment for treatments using different designs (columns) and antibiotic types (rows) for different mutation rates (x-axis). Colour and line-type indicate the magnitude of reciprocal CS simulated. The error bars represent the standard error of the estimation.

Discussion

Our analysis shows that CS can be exploited to design treatment schedules that suppress antibiotic resistance, where CS-based treatments hold the most potential for antibiotics with narrow-therapeutic windows. Our modelling approach indicated that several factors need to be considered to ensure optimal design of CS-based dosing regimens, which include antibiotic PD characteristics, the magnitude and reciprocity of CS effects, and the effect of fitness costs, and we found that the antibiotic sequence is of importance for the success of CS-based cycling treatments.

CS-based dosing schedules have mainly considered reciprocal CS scenarios, where resistance against one antibiotic leads to increased sensitivity and vice versa[12,16]. We show, however, that one directional CS can be sufficient to supress resistance. For a one-day cycling regimen, the one-directional CS effects were nearly identical to the scenario that considered reciprocal CS (**Figure 5A vs 5B**), but only when bacteria showed CS to the second drug administrated. In the case where CS was only present for the first antibiotic (AB_A) (**Figure 5D**), the initial bacterial growth was extensive, thus leading to increased risk of the double resistant subpopulation emerging. We consider this finding relevant because one-directional CS relationships are much more common than reciprocal CS relationships [9–16], thus expanding the number of clinical scenarios for which CS-based treatments can be designed.

We find that CS-based treatments show the greatest promise for antibiotics with narrow therapeutic window. The therapeutic window of an antibiotic is defined by the drug exposure, or concentration range, leading to sufficient efficacy while not leading to toxicity. In the majority of our simulations, we have studied dosing schedules leading to an antibiotic steady state concentrations (C_{ss}) of 1.5xMIC, which led to full kill of the sensitive population but did allow emergence of resistance to occur. This concentration can be considered to reflect a narrow-therapeutic window antibiotic, *e.g.,* where the antibiotic concentration required for bacterial killing is closer to the MIC because of occurrence of (severe) toxicities at higher concentrations. Indeed, for concentrations (much) higher than the MIC, the benefit of CS rapidly disappears (**Figure 7**). This means that in particular for antibiotics with a narrow therapeutic windows such as polymyxins or aminoglycosides, the relevance of CS-based dosing schedules is most significant.

Cycling based dosing regimens are frequently discussed as a strategy to utilize when CS occurs. We show that for one-day cycling treatments antibiotic type (**Figure 6**), directionality of CS (**Figure 5**), and the identity of any pre-existing resistance subpopulation (**Figure 9**) should be considered when choosing which drug to initiate therapy with. We find that the type of the first administrated antibiotic had a larger impact on the PoR compared to the type of the second administrated antibiotic, the presences of CS to the second administrated antibiotic had a greater effect PoR compared to CS to the first administrated antibiotic, and the PoR was smaller if there was pre-existing resistance to the second administrated drug compared to the first antibiotic. These findings are in line with previous studies which show that the probability of resistance development is influenced by the sequence of antibiotics[31], and optimized cycling sequences outperformed random drug cycling regimens [13]. Furthermore, in the context of cycling, or alternating antibiotic treatments, consideration of the pharmacokinetics, e.g. the time-varying antibiotic concentrations was found to be of importance because remaining concentration of the first antibiotic administered add to the total drug effect. Therefore, the antibiotic switch contributes to a higher total drug effect than after repeated administration of

the same drug**.** In our simulations, the impact of this increased effect is dependent on the type of the antibiotic and was shown to be especially important for time-dependent antibiotics.

To better characterize the population dynamics of pathogens in response to antibiotic treatment under presence of CS, we studied the effect of fitness costs of antibiotic resistance and mutation rates leading to antibiotic resistance. We find that the introduction of fitness cost had negligible effect on PoR for the majority of the simulated CS-based treatments, with the exception of the three-day cycling using time dependent antibiotics (**Figure 8J and 8N**), where the introduction of fitness cost improved the CS-based treatments because it prevents resistant bacteria to reach high levels before the first antibiotic switch. Pathogens with a low mutation rate (10^{-9}), one-day cycling regimens are most relevant to benefit from CS, whereas for high mutation rates (*e.g.,* 10^{-6}), sequential or simultaneous antibiotic treatments are most beneficial (**Figure 10**). This means that in situations when the occurrence of hypermutator strains is likely, *e.g.*, such as in CF [32], this should be considered in the design of dosing schedules. With respect to the competition between different bacterial subpopulations occurring *in vivo*, we included a bacterial carrying capacity which introduces clonal competition. During clonal competition, competition between subpopulations can lead to their suppression, *e.g.*, high densities for one subpopulation can suppress the growth of a second subpopulation, even if the second population might be more fit. When CS is present, single resistant subpopulations are unable to reach high enough levels to suppress the growth of the double resistant mutant, which allows the double mutant to take over, for some treatments.

Udekwu *et al*[33] previously demonstrated the utility of mathematical modelling to study cycling schedules for CS to delay emergence of antibiotic resistance *in silico*, simulating an *in vitro* chemostat experimental system, identifying the cycling interval to be the main factor impacting resistance development, and we consider this work as an important foundation of our study. Our study advances the work by Udekwu by explicitly comparing treatment outcomes to a base scenario without CS to determine the specific contribution of CS effects, and we perform a more systematic analysis of key drug- and pathogen specific factors that could influence optimal CS-based treatment scenarios.

Our mathematical model was designed to facilitate identification of the primary factors driving the success or failure of antibiotic treatments in a general setting, and not for specific antibiotics or pathogens. We thereby did not consider factors that could further contribute to treatment outcomes for specific pathogens or antibiotics. We did not consider more complex evolutionary mutational trajectories can occur with associated complex patters of changes in antibiotic sensitivity and MIC[36], which are not easily definable to apply to antibiotic treatment in general. Other factors not considered include local antibiotic tissue concentrations [34,35], pharmacodynamic drug-drug interactions or the contribution of the immune system. We expect that such factors will not affect specific subpopulations studied in different ways and therefore not have a great impact on the general findings we do in this analysis. The developed modelling framework is applicable for design of clinical treatment designs for specific antibiotic agents and pathogens, where the model can be further expanded with additional pathogen-, drug-, and patient-specific characteristics[37], derived from separate experimental studies and by utilizing published clinical population PK models for specific antibiotics[38,39], which include inter-individual variability or target site concentrations at the site of infection. This would thus allow to derive tailored CS-based dosing regimens for specific antibiotics and pathogens.

We conclude that CS-based treatments are likely to be able to contribute in the suppression of resistance. However, the success of such treatment strategies will be dependent on careful design of a dosing schedule, and requires explicit consideration of pathogen- and drug-specific characteristics. Our developed modelling framework can be of use to facilitate the design of such treatment. In addition, the robustness of such CS effects is another external factor that remains a key requirement, although reciprocal CS may not be a requirement to design such dosing schedules. CS treatments appear to be most relevant for antibiotics with a narrow therapeutic index, which are also the antibiotics where within-host emergence of resistance is most likely to occur.

Acknowledgements

We wish to acknowledge Hadi Taghvafard for helpful mathematical input and Laura Zwep for valuable discussions.

Competing interests

No competing interest to declare.

References

1. Luepke KH, Suda KJ, Boucher H, Russo RL, Bonney MW, Hunt TD, et al. Past, Present, and Future of Antibacterial Economics: Increasing Bacterial Resistance, Limited Antibiotic Pipeline, and Societal Implications. Pharmacotherapy. 2017;

2. Mcgrath DM, Qin X, Mojica MF, Miller C, Diaz L, Sc B, et al. Genetic Basis for In Vivo Daptomycin Resistance in Enterococci. n engl j med. 2011;365:892–900.

3. Mwangi MM, Wu SW, Zhou Y, Sieradzki K, Lencastre H De, Richardson P, et al. Tracking the in vivo evolution of multidrug resistance in Staphylococcus aureus by whole-genome sequencing. Proc Natl Acad Sci U S A. 2007;104(22):9451–6.

4. Nielsen EI, Friberg LE. Pharmacokinetic-pharmacodynamic modeling of antibacterial drugs. Pharmacol Rev. 2013;65(3):1053–90.

5. Bonhoeffer S, Lipsitch M, Levin BR. Evaluating treatment protocols to prevent antibiotic resistance. Proc Natl Acad Sci U S A. 1997;94(22):12106–11.

6. Baym M, Stone LK, Kishony R. Multidrug evolutionary strategies to reverse antibiotic resistance. Science (80-). 2016;351(6268):aad3292–aad3292.

7. Imamovic L, Sommer MOA. Use of collateral sensitivity networks to design drug cycling\nprotocols that avoid resistance development. Sci Transl Med. 2013;5(204):204ra132.

8. Lejla Imamovic A, Mostafa Hashim Ellabaan M, Manuel Dantas Machado A, Molin S, Krogh Johansen H, Otto Alexander Sommer M, et al. Drug-Driven Phenotypic Convergence Supports Rational Treatment Strategies of Chronic Infections. Cell. 2018;172:121–34.

9. Podnecky NL, Fredheim EGA, Kloos J, Sørum V, Primicerio R, Roberts AP, et al. Conserved collateral antibiotic susceptibility networks in diverse clinical strains of Escherichia coli. Nat Commun [Internet]. 2018;9(1):3673. Available from: https://doi.org/10.1038/s41467-018-06143-y

10. Barbosa C, Römhild R, Rosenstiel P, Schulenburg H. Evolutionary stability of collateral sensitivity to antibiotics in the model pathogen Pseudomonas aeruginosa. Elife [Internet]. 2019 Oct 29;8:1–22. Available from: https://elifesciences.org/articles/51481

11. Gonzales PR, Pesesky MW, Bouley R, Ballard A, Biddy BA, Suckow MA, et al. Synergistic, collaterally sensitive β-lactam combinations suppress resistance in MRSA. Nat Chem Biol. 2015;11(11):855–61.

12. Imamovic L, Sommer MOA. Use of collateral sensitivity networks to design drug cycling protocols that avoid resistance development. Sci Transl Med. 2013;5(204).

13. Maltas J, Wood KB. Pervasive and diverse collateral sensitivity profiles inform optimal strategies to limit antibiotic resistance. Schulenburg H, editor. PLOS Biol [Internet]. 2019 Oct 25;17(10):e3000515. Available from: https://dx.plos.org/10.1371/journal.pbio.3000515

14. Barbosa C, Trebosc V, Kemmer C, Rosenstiel P, Beardmore R, Schulenburg H, et al. Alternative Evolutionary Paths to Bacterial Antibiotic Resistance Cause Distinct Collateral Effects. Mol Biol Evol. 2017;34(9):2229–44.

15. Liakopoulos A, Aulin LBS, Buffoni M, van Hasselt JGC, Rozen DE. Allele-specific collateral and fitness effects determine the dynamics of fluoroquinolone-resistance evolution. bioRxiv [Internet]. 2020 Jan 1;2020.10.19.345058. Available from: http://biorxiv.org/content/early/2020/10/19/2020.10.19.345058.abstract

16. Kim S, Lieberman TD, Kishony R. Alternating antibiotic treatments constrain evolutionary paths to multidrug resistance. Proc Natl Acad Sci [Internet]. 2014 Oct 7;111(40):14494–9. Available from: http://www.pnas.org/content/111/40/14494.abstract

17. Regoes RR, Wiuff C, Zappala RM, Garner KN, Baquero F, Levin BR. Pharmacodynamic Functions: a Multiparameter Approach to the Design of Antibiotic Treatment Regimens. Antimicrob Agents Chemother. 2004;48(10):3670–6.

18. Coen Van Hasselt JG, Iyengar R. Systems pharmacology: Defining the interactions of drug combinations. Annu Rev Pharmacol Toxicol. 2019;59:21–40.

19. Pál C, Papp B, Lázár V. Collateral sensitivity of antibiotic-resistant microbes. Trends Microbiol. 2015;23(7):401–7.

20. Sharma R, Sharma S. Physiology , Blood Volume. Vol. l, StatPearls. 2020. p. 6–9.

21. Gerlini A, Colomba L, Furi L, Braccini T, Manso AS, Pammolli A, et al. The Role of Host and Microbial Factors in the Pathogenesis of Pneumococcal Bacteraemia Arising from a Single Bacterial Cell Bottleneck. 2014;10(3).

22. Martínez JL, Baquero F. Mutation Frequencies and Antibiotic Resistance. Antimicrob Agents Chemother. 2000;44(7):1771–7.

23. Wang W, Hallow KM, James DA. A Tutorial on RxODE : Simulating Differential Equation Pharmacometric Models in R. 2016;(August 2015):3–10.

24. Fidler M, Hallow M, Wilkins J WW. RxODE: Facilities for Simulating from ODE-Based Models. R package version 1.0.6 [Internet]. 2021. Available from: https://cran.r-project.org/package=RxODE

25. Falagas ME, Kasiakou SK. Toxicity of polymyxins: A systematic review of the evidence from old and recent studies. Crit Care. 2006;10(1).

26. Mattie H, Craig WA, Pechere JC. Determinants of efficacy and toxicity of aminoglycosides. J Antibiot (Tokyo). 1989;24:281–93.

27. Zasowski EJ, Murray KP, Trinh TD, Finch NA, Pogue JM, Mynatt RP. crossm Identification of Vancomycin Exposure-Toxicity Thresholds in Hospitalized Patients Receiving Intravenous Vancomycin. Antimicrob Agents Chemother. 2018;62(1):e01684-17.

28. Andersson DI, Hughes D. Antibiotic resistance and its cost : is it possible to reverse resistance ? Nat Rev Microbiol. 2010;8.

29. Band VI, Crispell EK, Napier BA, Herrera CM, Tharp GK, Vavikolanu K, et al. Antibiotic failure mediated by a resistant subpopulation in Enterobacter cloacae. Nat Microbiol. 2016;1:16053.

30. Long H, Miller SF, Strauss C, Zhao C, Cheng L, Ye Z, et al. Antibiotic treatment enhances the genome-wide mutation rate of target cells. 2016;

31. Nichol D, Jeavons P, Fletcher AG, Bonomo RA, Maini PK, Paul JL, et al. Steering Evolution with Sequential

546 Therapy to Prevent the Emergence of Bacterial Antibiotic Resistance. Antia R, editor. PLOS Comput Biol
547 [Internet]. 2015 Sep 11;11(9):e1004493. Available from: https://dx.plos.org/10.1371/journal.pcbi.1004493

548 32. Looft C, Reinsch N, Rudat I, Kalm E, Sel G, Chardon P, et al. High Frequency of Hypermutable Pseudomonas
549 aeruginosa in Cystic Fibrosis Lung Infection. Science (80-). 2000;288(5469):1251–4.

550 33. Udekwu KI, Weiss H. Pharmacodynamic considerations of collateral sensitivity in design of antibiotic treatment
551 regimen. Drug Des Devel Ther [Internet]. 2018 Jul;Volume 12:2249–57. Available from:
552 https://www.dovepress.com/pharmacodynamic-considerations-of-collateral-sensitivity-in-design-of--peer-
553 reviewed-article-DDDT

554 34. Välitalo PAJ, Griffioen K, Rizk ML, Visser SAG, Danhof M, Rao G, et al. Structure-Based Prediction of Anti-
555 infective Drug Concentrations in the Human Lung Epithelial Lining Fluid. Pharm Res. 2016;856–67.

556 35. Aulin LBS, Valitalo PA, Rizk ML, Visser SAG, Rao G, Graaf PH Van Der, et al. Validation of a Model Predicting
557 Anti-infective Lung Penetration in the Epithelial Lining Fluid of Humans. Pharm Res. 2018;6–9.

558 36. Aulin LBS, Koumans CIM, Haakman Y, van Os W, Kraakman MEM, Gooskens J, et al. Distinct evolution of colistin
559 resistance associated with experimental resistance evolution models in Klebsiella pneumoniae. J Antimicrob
560 Chemother. 2020;1–3.

561 37. Aulin LBS, Lange DW, Saleh MAA, Graaf PH, Völler S, Hasselt JGC. Biomarker-Guided Individualization of
562 Antibiotic Therapy. Clin Pharmacol Ther [Internet]. 2021 Mar 2;0(0):cpt.2194. Available from:
563 https://onlinelibrary.wiley.com/doi/10.1002/cpt.2194

564 38. Aulin LBS, De Paepe P, Dhont E, de Jaeger A, Vande Walle J, Vandenberghe W, et al. Population
565 Pharmacokinetics of Unbound and Total Teicoplanin in Critically Ill Pediatric Patients. Clin Pharmacokinet
566 [Internet]. 2020;(0123456789). Available from: https://doi.org/10.1007/s40262-020-00945-4

567 39. Cock PAJG De, Mulla H, Desmet S, Somer F De, Mcwhinney BC, Ungerer JPJ, et al. Population pharmacokinetics
568 of cefazolin before , during and after cardiopulmonary bypass to optimize dosing regimens for children
569 undergoing cardiac surgery. J Antimicrob Chemother. 2017;72:791–800.

570

571

Supplementary figures

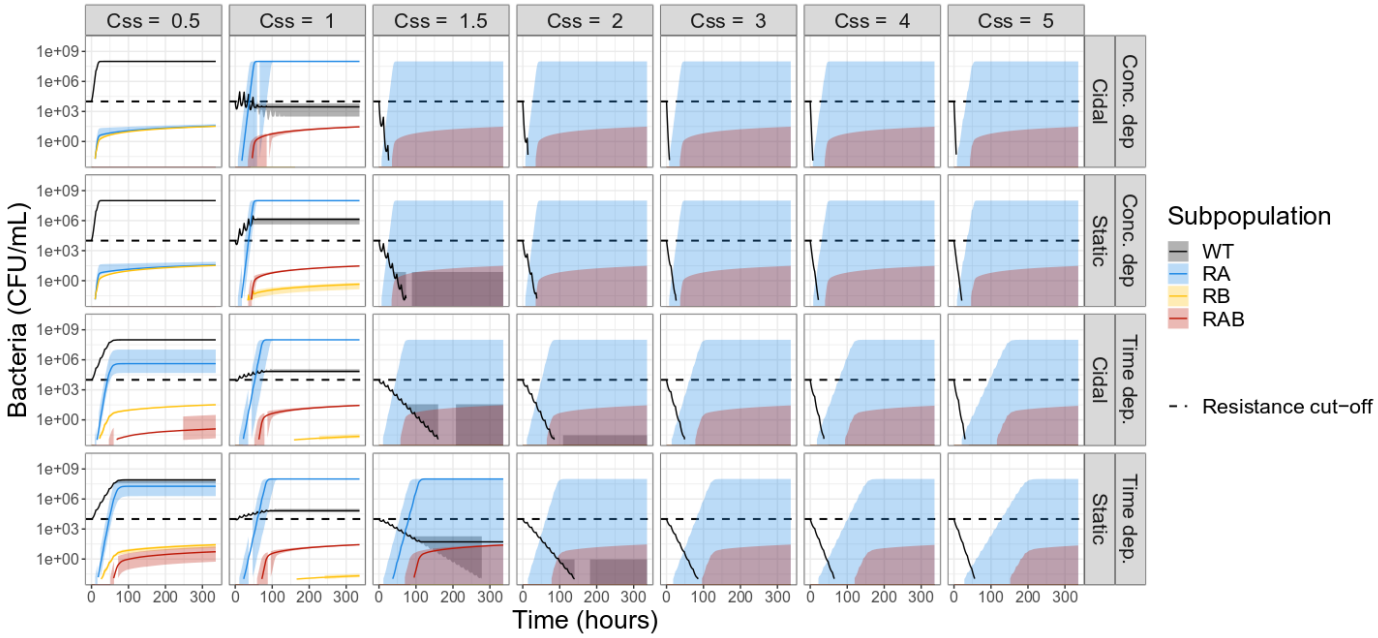

Figure S1. Bacterial dynamics for simulated monotherapy using different antibiotic types (rows) and steady state concentrations (Css) relating to the MIC of the wild type (WT) (columns). These simulations shows that monotherapy required C_{ss} equal to 1.5 x MIC_{WT} to achieve killing of the WT, regardless of the drug type used. Subpopulation-specific bacterial density are indicated by different colures, where the solid lines indicate the median and the shaded area covers the 5^{th}-95^{th} percentiles of the predictions. The resistance cut-off (dashed line) is used for end of treatment evaluation of resistance.

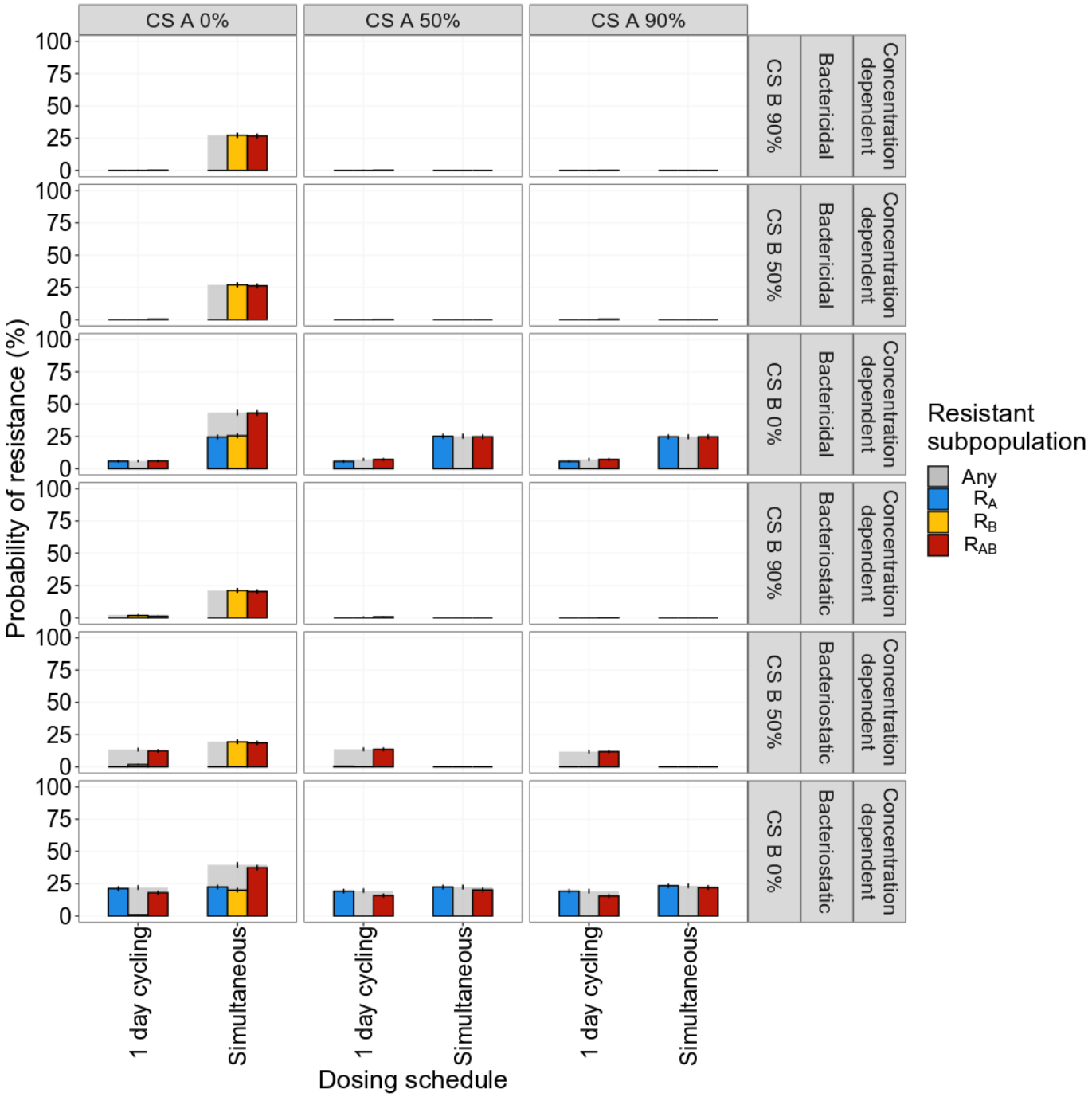

Figure S2. The effect of the direction or reciprocally of collateral sensitivity (CS) on end of treatment probability of resistance (PoR). PoR was estimated at end of treatment for different CS scenarios using concentration dependent bacteriostatic or bactericidal drugs. Subpopulation-specific PoR is indicated by different colour and R_{Any} resistance, defined as the presence of any resistant subpopulation, is indicated in grey. The error bars represent the standard error of the estimation of PoR. For the one-day cycling regimen it became evident that the CS towards the second administrated drug (AB_B) was driving the effect, CS-based dosing using simulations administration of concentration dependent antibiotics showed that reciprocity is necessary to supress overall resistance.

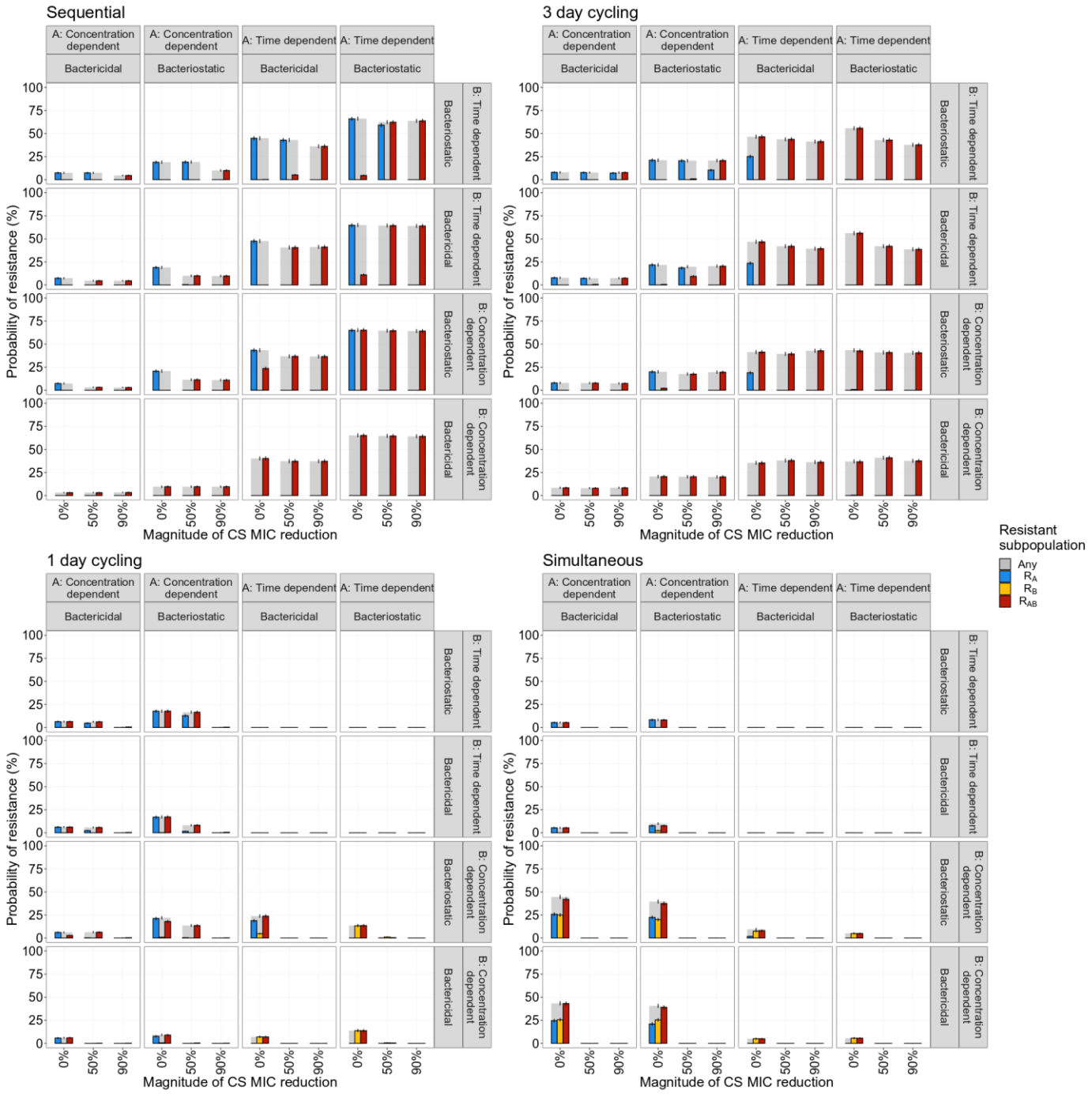

Figure S3. The effect of using different antibiotic combinations during treatments in relation to different levels of collateral sensitivity (CS) on the probability of resistance (PoR) at the end of treatment. PoR was estimated at the end of treatment for different treatment schedules with different antibiotic combinations. Subpopulation-specific PoR is indicated by different colour and R_{Any}, defined as the presence of any resistant subpopulation, is indicated in grey. The error bars represent the standard error of the estimation of PoR.

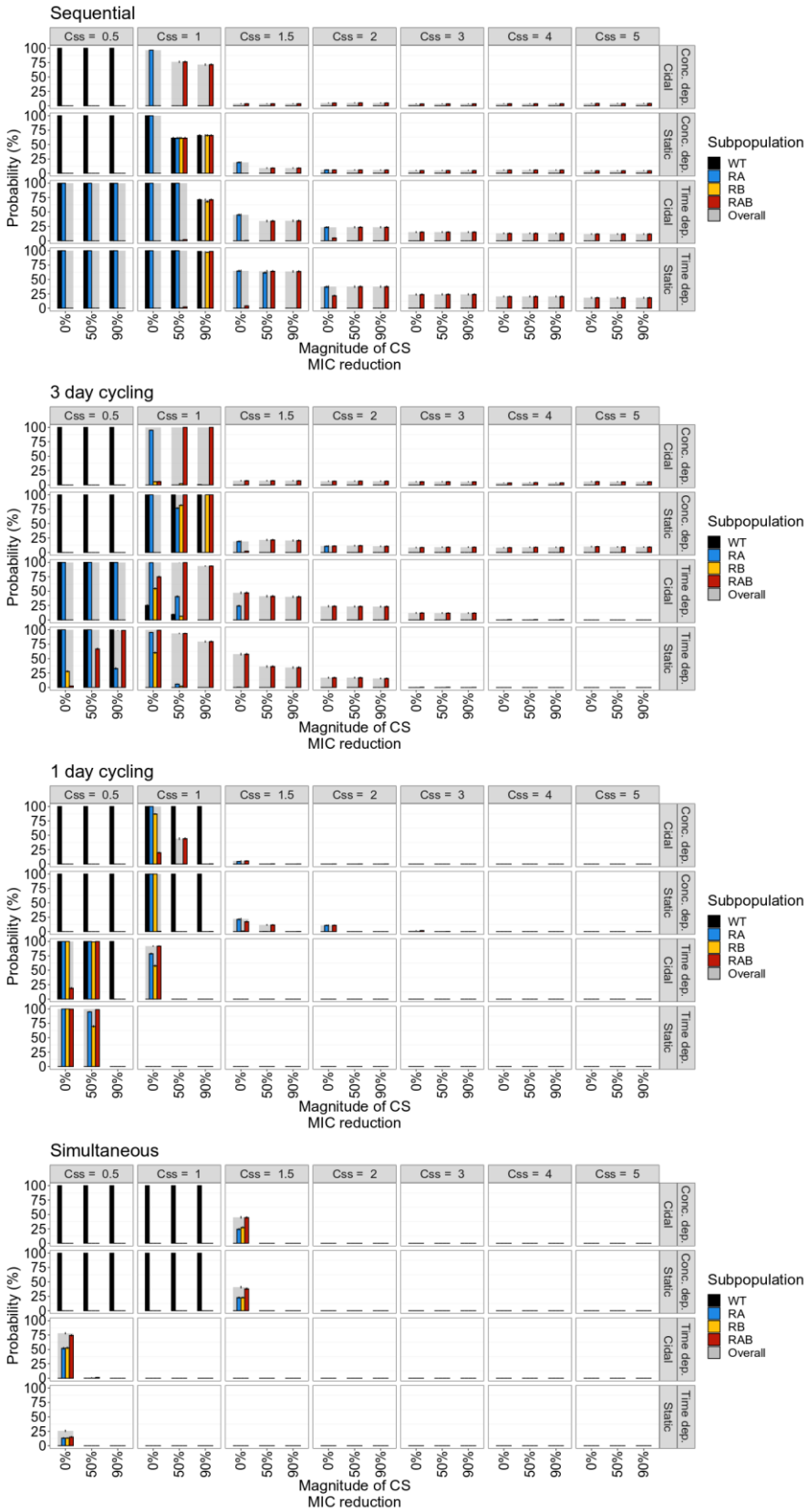

Figure S4. The effect of antibiotic steady state concentrations (C_{ss}) in relation to different levels of collateral sensitivity (CS) on the probability of resistance at the end of treatment (PoR). C_{ss} was expressed as factor difference from the MIC_{WT}. PoR of R_{Any}, defined as the presence of any resistant subpopulation, was estimated at the end of treatment for treatments using different designs and antibiotic types (rows). Subpopulation-specific PoR is indicated by different colour and R_{Any} is indicated in grey. The error bars represent the standard error of the estimation of PoR.

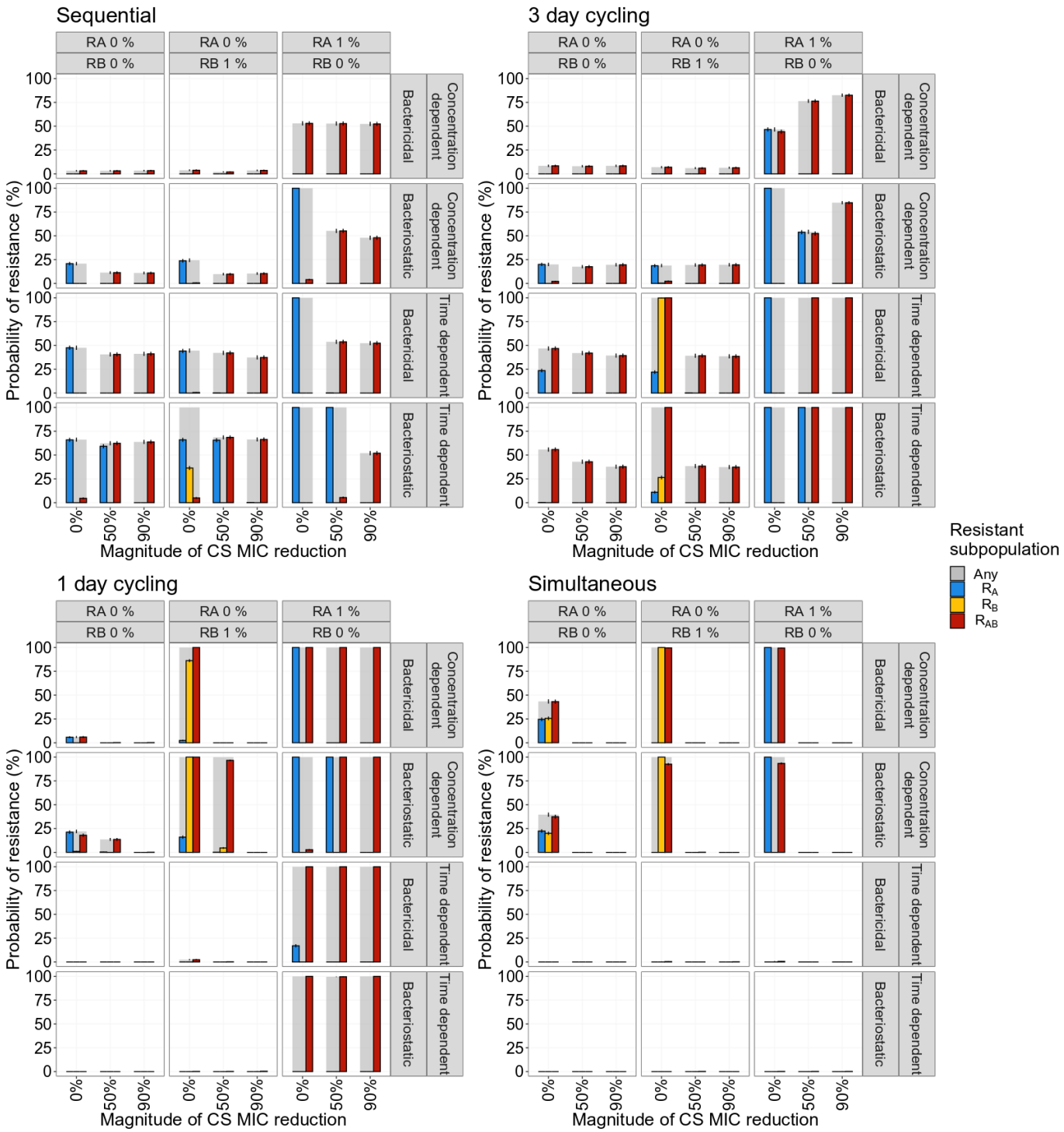

Figure S5. The effect of pre-existing resistant mutants for different magnitudes of collateral sensitivity on the probability of resistance (PoR). PoR was estimated at the end of treatment for different scenarios of low levels of pre-existing resistance (columns) and antibiotic types (rows). Subpopulation-specific probability of resistance is indicated by colour and PoR of R_{Any}, defined as the presence of any resistant subpopulation, is indicated in grey. The error bars represent the standard error of the estimation of PoR.